Fermilab

AP-Note-90-001

ACCELERATOR PHYSICS DEPARTMENT

AP Note 90-001

TITLE: The driven pendulum without action-angle variables: Order, chaos and more

AUTHOR: George P. Tsironis

March, 1990

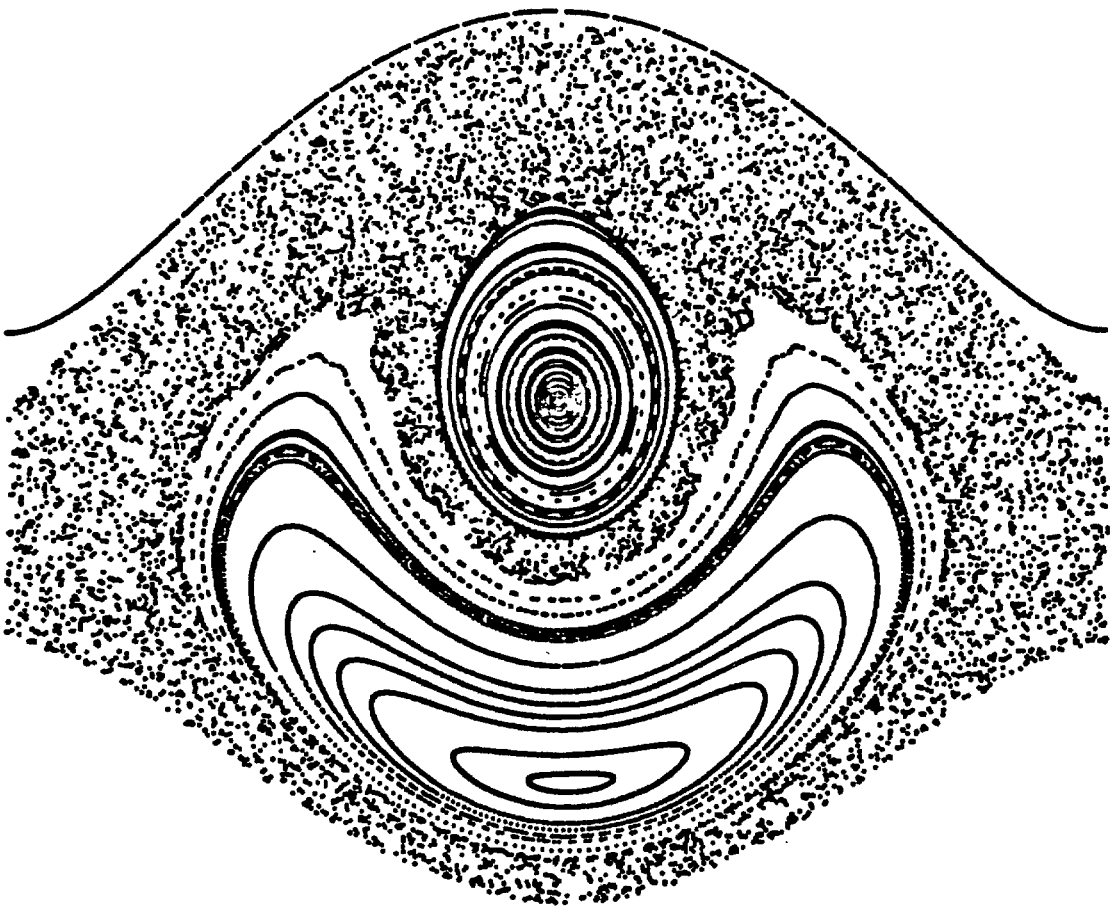

AP Note 90-001

THE DRIVEN PENDULUM WITHOUT ACTION-ANGLE VARIABLES: ORDER, CHAOS AND MORE

George P. Tsironis

Fermi National Accelerator Laboratory
Batavia, IL 60510

January, 1990

1 Introduction

In this note we deal with the driven pendulum, its variants and an application to accelerators. We are mostly interested in describing some analytic and perturbative solutions that can be obtained relatively easily and can be used as a guide in a more complete study of the driven pendulum. In a sense this note contains all the "standard" pendulum formulas and can be used as a reference or starting point for future work. We also added an appendix on elliptic integrals and elliptic functions that are extremely useful in the study of nonlinear problems.

One of the issues of critical importance in accelerator physics applications is the knowledge of the boundary that separates regular and chaotic motion. The reason for this is very simple and rather obvious. When particles are in the chaotic region their dynamics is erratic and ultimately escape to infinity. Since the pendulum study is very closely related to the dynamics of particles in an accelerator[1] it is essential to know the location of the surface in phase space that separates different types of pendulum dynamics. In this note we derive some results that are related to the possible types of pendulum motion as a function of driving frequency and amplitude. In particular a new

formula is obtained for the boundary that separates regular and stochastic pendulum motion. This expression, calculated to lowest order in the pendulum amplitude, improves on a similar expression given in ref. [1]. The latter is strictly valid in the linearized pendulum whereas we arrive at the former without linearizing the equation of motion. We also present numerical results that show preliminary agreement with these ideas.

We use the following equation of motion:

$$\frac{d^2\psi}{dt^2} + \omega_0{}^2 sin\psi = \epsilon sin(\Omega t), \tag{1}$$

where ω_0 is the frequency of small oscillations, Ω is the driving frequency and ϵ is the amplitude of the driving torque. This equation appears in nonlinear beam dynamics situations with time dependent perturbations. In that context the parameters in Eq. (1) are related to quantities in the real accelerator. Following Peggs[1], we have (near a fifth order resonance):

$$\psi = 5\phi, \tag{2}$$

$$\omega_0 = 2\pi Q_I, \tag{3}$$

$$\Omega = 2\pi Q_M, \tag{4}$$

$$\epsilon = 5(2\pi)^2 q Q_M, \tag{5}$$

with Q_M the tune of the mashine. For more details on how these realations arise, see reference [1].

2 Small-angle nonlinear dynamics

For very small angles the driven pendulum equation reduces to the equation of a harmonic oscillator with natural frequency ω_0. In this case we have the well known phenomenon of *resonance*, viz. when the external driving frequency Ω is equal to ω_0 the oscillator amplitude diverges. This divergernce is an artifact of the approximation. For, let us assume that we place initially the pendulum at a very small angle and drive it at the frequency $\Omega = \omega_0$ with small driving amplitudes ϵ. Then, since the angle is small, the pendulum responds in a resonant fashion to the external force and the angle $\psi(t)$ increases rapidly. As this happens however, the pendulum experiences

the nonlinear parts of its periodic potential and the diverging motion is suppressed. This suppression is caused by the changes in the force as a function of angle. We thus expect the following motion for the pendulum: At first, small oscillations with increasing amplitude. As we pass beyond the linear regime the rate of increase of the amplitude decreases and finally stops. The pendulum then, under the action of gravity "rolls" back towards the equilibrium point with increasing rate in the amplitude decreases. As it reaches the linear regime, it feels again the resonating driving frequency and the cycle repeats itself.

From the qualitative discussion we see that the phenomenon of resonance is far more complicated in a nonlinear system than in a linear one. One immediate conclusion is that a shift is expected in the resonance frequency in the nonlinear case for very small driving amplitudes ϵ. We expect this shift to be towards smaller frequencies, i.e. the *nonlinear resonance* occurs at the driving frequency Ω_{res} with $\Omega_{res} < w$. The reason for the shift in this direction is the following: Assume that the nonlinear pendulum motion that is bounded between angles $-\frac{\pi}{2} \leq \psi \leq \frac{\pi}{2}$ can be described by a corresponding quadratic *renormalized* potential. The resonant frequency for this oscillator would be

$$\Omega_{res} = \omega\sqrt{\kappa_{ren}} = \omega_0\sqrt{< \frac{sin\psi}{\psi} >} \tag{6}$$

The renormalization coefficient κ takes into account in some average way the nonlinearity of the potential. The function $sinx/x$ is a decreasing function in the range we are interested in. Were we to assume linear distribution in x with a reasonable cutoff for the linear regime, i.e. $x_{cut} \simeq 0.52$ corresponding to an angle of 30°, then

$$\kappa_{ren} = \sqrt{< \frac{sinx}{x} >} \approx cos(x_{cut}) \approx 0.930 \tag{7}$$

This then shows that the new resonant frequency occurs typically for smaller frequencies than ω_0.

In the remaining of this section we will explore some useful aspects of an approximate yet nonlinear equation for the motion of the pendulum. First we will study the pendulum with no driving force and then we will apply some of the intuition and results obtained to the driven pendulum.

2.1 Approximate solutions

When $\epsilon = 0$, Eq. (1) reduces to the equation for a free pendulum. The physical characteristics of the solution depend on the total energy of the pendulum, i.e. depends on the intial conditions. For small amplitude oscillations the *sin*-function can be approximated by $sin(\psi) \approx \psi$ and the pendulum executes small oscillations with constant frequency ω_0 independent of the (small) amplitude. For larger inital amplitudes (or total energy) this approximation is no longer valid. Let us go to the next order term in the expanssion, viz.

$$sin\psi \approx \psi - \frac{\psi^3}{3!}. \tag{8}$$

We now have the following nonlinear equation of motion:

$$\frac{d^2\psi}{dt^2} + \omega_0{}^2(\psi - \frac{\psi^3}{6}) = 0 \tag{9}$$

This is nothing but the equation of motion for a classical particle moving with rescaled time $\tau = \omega_0 t$ in an *inverted* double well potential given by

$$V(\psi) = \frac{\psi^2}{2} - \frac{\psi^4}{24}. \tag{10}$$

Note that the zeros of $V(\psi)$ are at $\psi_{zero} = 0$ (double) and $\psi_{zero} = \pm\sqrt{12} \approx \pm 3.46410$ and there is a maximum at $\psi_{max} = \pm\sqrt{6} \approx \pm 2.44949$. Since ψ is an angle measured in radians the value ψ_{max} corresponds to an angle of approximately 140.35°. Clearly, for intial angles as large as 140° the approximation breaks down and the motion in the approximate equation becomes unstable. In fact, to be on the safe side, we should not really use the approximate nonlinear equation for parts of the potential where the curvature is negative. The second derivative of the potential changes sign at $\psi_{cur} = \pm\sqrt{2} \approx \pm 1.41421$ corresponding to an angle of 81.028°. Thus our approximate equation is good, roughly speaking, for the range $-80° \leq \psi \leq +80°$. Now we control fully the regime of validity of our approximations we can go on and attempt solving the approximate equation.

To simplify matters, we will fix the initial conditions. Let us assume that we initially displace the particle by ψ_o and then simply "drop" it with no

initial momentum, i.e. take $\dot{\psi}_o \equiv p_0 = 0$. The particle (or pendulum) will then execute oscillations between $-\psi_o$ and ψ_o with time evolution given by

$$\psi(t) = a_1 cos(\omega t) + a_3 cos(3\omega t) + \cdots \tag{11}$$

where the frequency ω depends on ω_0 *and* the initial conditions. If we now substitute Eq. (11) in the differential equation of Eq. (9) and keep only the fundamental and the first harmonic we get to lowest order:

$$\omega^2 = {\omega_0}^2[1 - \frac{3}{24}{a_1}^2 - \frac{1}{4}{a_3}^2], \tag{12}$$

$$a_3 = \frac{1}{24}\frac{1}{1 - 9\omega^2 - \frac{1}{2}}. \tag{13}$$

Assume an intial angle of approximately 60°, i.e. $\psi_0 \simeq 1$. Since this choice does not represent large deviations from the linear regime we will take initially $a_1 \approx \psi_0 = 1$ and $a_3 \simeq 0$. Substituting these numbers in Eqs. (12), (13) we have $\omega \approx 0.935\omega_0$ and $a_3 \simeq -5.6 \times 10^{-3}$. Using the new value for a_3, we obtain $a_1 \simeq 0.9944$, giving a ratio between the amplitudes of the harmonics equal to $a_1/a_3 \simeq 177$. We observe that the new "resonant" frequency shifts to the "red" and that more harmonics appear yet with much smaller strength.

2.2 Exact solutions

We now come to the exact solution of Eq. (9). We define $\tau = \omega_0 t$, multiply both sides of the equation with $\dot{\psi}$ and integrate once; we get

$$(\frac{d\psi}{d\tau})^2 + \psi^2 - \frac{\psi^4}{12} = C_0, \tag{14}$$

$$C_0 = p_0 + {\psi_0}^2 - \frac{{\psi_0}^4}{12} \tag{15}$$

where p_0, ψ_0 correspond to the initial momentum and angle respectively. To simplify the calculations we will take $p_0 = 0$. We now define two new quantities:

$$\lambda^2 = 1 - \frac{{\psi_0}^2}{12}, \tag{16}$$

$$k^2 = \frac{1 - \lambda^2}{\lambda^2} = \frac{\frac{{\psi_0}^2}{12}}{1 - \frac{{\psi_0}^2}{12}}, \tag{17}$$

and denote $w = \psi/\psi_0$. After some algebra the equation of motion in Eq. (14) simplifies considerably. We get

$$(\frac{dw}{d\lambda\tau})^2 = (1-w^2)(1-k^2w^2) \tag{18}$$

or equivalently

$$\int_1^w \frac{dw}{\sqrt{(1-w^2)(1-k^2w^4)}} = \lambda\tau \tag{19}$$

The elliptic integral on the left hand side of the equation defines the inverse of the *sn* Jacobian elliptic function with argument $w + K$ and modulus k. $K \equiv K(k)$ is the complete elliptic integral of the first kind with the same modulus. Equivalently, the solution can be written in terms of the *cd* elliptic function since:[2]

$$sn(u+K,k) = cd(u,k) = \frac{cn(u,k)}{dn(u,k)} \tag{20}$$

Finally the solution of Eq. (14) is given by

$$\psi(\tau) = \psi_0 cd(\lambda\tau,k) = \psi_0 \frac{cn(\lambda\tau,k)}{dn(\lambda\tau,k)} \tag{21}$$

with λ and k defined in Eq. (16). The Jacobian elliptic functions that describe the motion of the pendulum are periodic functions. In particular, the (real) period of *cd* is $4K$.

Of interest to us here is also the Fourier spectrum of the pendulum motion. Since elliptic funtions are periodic, they can be expanded in Fourier series. In the case of the *cd* Jacobian function we have[2]

$$cd(u,k) = \frac{2\pi}{kK}\sum_{n=0}^{\infty}(-1)^n \frac{q^{n+\frac{1}{2}}}{1-q^{2n+1}} cos[(2n+1)\frac{\pi u}{2K}, \tag{22}$$

$$q = exp[-\pi\frac{K'}{K}] \tag{23}$$

where $K' \equiv K(k') = K(\sqrt{1-k^2})$ and q is called the *nome*. In the pendulum case, the new frequencies are given by

$$\omega'_{2n+1} = (2n+1)\frac{\pi}{2K(k)}\lambda\omega_o \tag{24}$$

Using standard tables for elliptic integrals we can evaluate the first few frequencies and their relative strengths. We have for the new fundamental

$$\omega_1 \simeq 0.935\omega_0 \tag{25}$$

Note that this is identical to the new frequency value obtained previously using an approximate approach. The relative strength of the first two lines is approximately $a_1/a_3 \simeq 170$ for initial amplitudes $\psi \simeq 1$, compatible with the approximate results. The frequency spacing between Fourier lines depends on the initial conditions. In fact it decreases rapidly as the intial amplitude increases. As this happens the potential becomes more nonlinear and higher harmonics are necessary for a satisfactory description of the motion.[3]

2.3 Driven motion

We now come to the study of the equation with cubic nonlinearity driven by the *periodic force. The equation of motion is*

$$\frac{d^2\psi}{dt^2} + \omega_0{}^2(\psi - \frac{\psi^3}{6}) = \epsilon sin(\Omega t). \tag{26}$$

It describes a large range of possible dynamic evolution. Since we ultimately want to study sidebands in the accelerator we are mostly interested in solutions where the free oscilltions are not important. We thus look for solutions of the type

$$\psi(t) = \alpha sin(\Omega t) \tag{27}$$

Substituting Eq. (27) into Eq. (26) and keeping only the lowest order terms we arrive at the following compatibility equation

$$-\alpha(\Omega)^2 + \alpha\omega_0{}^2[1 - \frac{1}{8}\alpha^2] = \epsilon \tag{28}$$

This equation essentially describes a *nonlinear resonance.* Note that if the nonlinear term was absent from Eq. (26), the equation above would give the amplitude of oscillatory motion as a function of driving amplitude and frequency. In this case, when $\Omega = \omega_0$ the amplitude diverges and we have a (linear) resonance.

There is a variety of things we can learn from E. (28). For now, we restrict our attention to only one: For a given amplitude α we can find the critical

line that separates stable periodic motion for that amplitude (or less) and unstable motion. In particular, we obtain the frequency shift of the resonant point as $\epsilon \to 0$. It is given by

$$\Omega^2 = \omega_0{}^2[(1 - \frac{1}{8}\alpha^2)] \tag{29}$$

Clearly, when α is very small, there is no frequency shift. As the amplitude becomes larger we have a red frequency shift. For instance for $\alpha = 1$ we get once again $\Omega \simeq 0.935\omega_0$. In Fig. 1 we plot ϵ vs Ω for $\alpha = 1$ (Fig. 1a), $\alpha = 2$ (Fig. 1b) and compare it with the linear result (dotted line)[1].

3 Exact nonlinear dynamics and resonances

We now turn to the full scale study of the pendulum for arbitrary amplitudes and no approximations in the equation of motion. The approximate solutions of the previous section are a useful guidance and they are certainly valid for reasonably small initial conditions. For $\epsilon = 0$ we get an equation which is exactly solvable in terms of elliptic functions. Unlike the small amplitude solution of section (2.2) this solution is a bit more complicated. This is because the pendulum now executes rotations in addition to oscillations. The rotations are superimposed to the free oscillations around the stable equilibrium point. A Fourier analysis of this solution shows an infinite number of lines, much like in the cubic case, superimposed to the running solutions.

The driven case is the most interesting one. There is a wealth of possible dynamics: oscillations with the driving frequency, rotations with a multiple of this frequency, chaotic transitions from one type of motion to the other, etc. It is not quite easy to clasify all the types of motion, even in an approximate fashion withough the use of digital simulations. In the remainder of this note we will do the following: First we solve the non-driven pendulum via elliptic functions and analyze the types of motion as well as the Fourier spectrum of the solution. We then try to find driven solutions to the pendulum. In doing that we obtain an equation similar to that of section (2.3) which we will use as the lowest order *nonlinear* approximant to the boundary that separates regular from stochastic regions. We will also present some simulation results that suport and put bounds to these results.

3.1 Exact free pendulum dynamics

The non-driven pendulum equation is

$$\frac{d^2\psi}{d\tau^2} + sin\psi = 0 \tag{30}$$

where $\tau = \omega_0 t$. We find the solution in steps: Introduce a new dependent variable θ through:

$$\psi = 2\theta \tag{31}$$

Using the trigonometric identity for the double angle and multiplying both sides of the equation by $\dot{\theta} \equiv d\theta/d\tau$ we get

$$\dot{\theta}\ddot{\theta} = -\dot{\theta} sin\theta cos\theta \tag{32}$$

or equivalently

$$\frac{1}{2}\frac{d}{d\tau}(\dot{\theta})^2 = \frac{1}{2}\frac{d}{d\tau}[k^2 - sin^2\theta] \tag{33}$$

with k^2 a constant of integration. For simplicity we now take the intial momentum to be zero. We thus have $k^2 = sin^2\theta_0$ and after integration we obtain

$$(\dot{\theta})^2 = k^2 - sin^2\theta \tag{34}$$

Next change to $y = sin\theta$ and Eq. (34) becomes

$$\dot{y}^2 = (k^2 - y^2)(1 - y^2) \tag{35}$$

Finally call w the ratio of y/k, viz. $w = y/k$ and we end up with an equation essentially identical to Eq. (18):

$$\int_1^w \frac{dw}{\sqrt{(1-w^2)(1-k^2w^4)}} = \tau \tag{36}$$

The solution to this equation is the *cd*- Jacobian elliptic function (Eq. (20)) with argument τ and modulus k. It is now a simple matter to write the solution in terms of the original vatiables. After "undoing" the transformations we get:

$$\psi(t) = 2arcsin[kcd(\omega_0 t, k)], \tag{37}$$

$$k = sin\frac{\psi_0}{2} \tag{38}$$

This is then the exact solution for the pendulum equation. For small initial amplitudes it reduces to the solution given in Eq. (21). Since our system is conservative and we assumed $p_0 = 0$ the angle in the solution above does not exceed 2π. It is relatively straigthforward to write the solution for $\dot{\psi}(\tau = 0) = p_0 \neq 0$ but $\psi(\tau = 0) = \psi_0 = 0$. We have in this case

$$\psi(t) = 2arcsin[ksn(\omega_0 t, k)], \tag{39}$$

$$k = p_0 \tag{40}$$

If $k^2 \geq 1$ we can use the identity $ksn(u,k) = sn(ku, 1/k)$ to obtain a more appropriate form for the solution:

$$\psi(t) = 2am[p_0\omega_0 t, \frac{1}{p_0}] \tag{41}$$

A Fourier analysis of the last equation leads to[2]

$$\psi(t) = \frac{\pi u}{K} + 4\sum_{n=0}^{\infty} \frac{q^{n+1}}{(n+1)[1+q^{2(n+1)}]} sin[(n+1)\frac{\pi u}{K}], \tag{42}$$

$$u = p_0\omega_0 t, \tag{43}$$

$$k = \frac{1}{p_0} \tag{44}$$

and q is the nome. The new frequencies of the oscillating part of the solution are

$$\omega_n' = (n+1)\frac{\pi}{K(\frac{1}{p_0})} p_0\omega_0 \tag{45}$$

Let us do a numerical example: For $p_0 = 1.1$ (rotations) we get

$$\omega_0{}' \equiv 8.05\omega_0 \tag{46}$$

as well as higher harmonics which are multiples of the new fundamental.

3.2 Driven pendulum

We finally come to the case of the driven pendulum with no approximations but no exact solutions either. It is well known that we now can have extreme

sencitivity on initial conditions or *chaos.* In this section we will attept the following tasks: Obtain approximate driven solutions in the spirit of section (2.3) and compare these perturbative yet analytic results with numerical simulations. The numerical integration of the driven pendulum is done in the code DPEND.

We need to know when driven pendulum motion with frequency identical to the driving frequency is possible. This can be found if we look for solutions of Eq. (1) of the form

$$\psi(t) = \alpha sin(\Omega t) \tag{47}$$

Solutions of this simple form can only be approximate ones since when we substitute Eq. (47) to Eq. (1) higher order odd harmonics appear. This follows easily from the identity[4]

$$sin[\alpha sin(\Omega t)] = 2\sum_{k=0}^{\infty} J_{2k+1}(\alpha) sin[(2k+1)\Omega t] \tag{48}$$

where $J_\nu(x)$ is a Bessel function of first kind. As a rule of thumb the values of these functions are very small for $x \geq \nu$. Since the maximum possible value of the angle α is of order $\pi \sim 3$ in the case of oscillations, we can safely ignore all but the first term in the sum. We thus have the following compatibility condition, analogous to Eq. (28):

$$-\alpha\Omega^2 + 2J_1(\alpha)\omega_0{}^2 = \epsilon \tag{49}$$

Note that Eq. (28) can be regained for small α since $J_1(\alpha) \simeq \alpha/2 - \alpha^3/16$.

The compatibility equation can be used in various ways: For given driving amplitude ϵ and frequency Ω we can determine maximum phase α. That can be done by numerically finding the roots of the equation. This maximum value for the oscillation should signal the transition from a periodic regime and thus a closed pendulum orbit to non periodic and presumably chaotic motion. This transition cannot be abrupt since the equation derived above is only an approximate one. However it should provide with a reasonably good estimate for the transition region. In addition, we can also determine the relationship between driving amplitudes and frequencies for various α's.

Since the main motivation of this analysis is to study the effect of periodic current fluctuations near an n-th order resonance in an accelerator we prefer

to turn now to the accelerator case. In the next section we will translate all our variables for the case of a fifth order resonance, write the analytical predictions in this language and test them against numerical simulations

4 Order and chaos in the accelerator

We are now in the position to discuss some preliminary tests of the theory. The numerical results are obtained with the code DPEND that integrates the differential equation of Eq. (1) or the corresponding mapping that derives from it. For our purposes we assume that these two discriptions are equivalent. Clearly there are cases where the differential equation approach is not a good approximation for an accelerator physics application but our case is not one of them. Since more complete results will be reported elsewhere, we restrict ourselves here in performing the following two tasks: First we test the predictions for the location of the nonlinear resonances for small driving amplitudes. This is accomplished through the study of the Poincaré surfaces of section which in our case are *strobe plots*. Second, we use a similar approach in order to test the validity of the equation for the boundary derived in section (3.2). In terms of the accelerator quantities given in Eqs. (2)-(4), Eq. (49) is

$$q\omega = \frac{Q_I}{5}[-\alpha\omega^2 + 2J_1(\alpha)], \tag{50}$$

$$\omega = \frac{Q_M}{Q_I} \tag{51}$$

Note that ω is now the ratio of the driving frequency to the tune of the accelerator. The factor *5* in the denominator on the rhs of Eq. (50) is indicative of the order of the resonance[1].

4.1 Nonlinear resonances

We take the noninteger part of the tune to be $Q_I = 0.0053$. Based on the theoretical results we expect for small enough q's the first resonance to be redshifted to $\omega \simeq 0.93$ or $Q_M \simeq 4.9 \times 10^{-3}$. The second resonance is weaker and appears at $\omega \simeq 2.80$ or $Q_M \simeq 1.3 \times 10^{-2}$. These figures change slightly

to smaller values if we make use of the amplitude dependent equation above (Eq. (50)). For instance for $\alpha \simeq 2$ we get $Q_M \simeq 4.6 \times 10^{-3}$.

In Figs. 2, 3 we present a series of strobe plots for a small number of intial conditions (fifteen in total) that launch the pendulum initially with different angles but zero initial momentum. We vary the driving frequency Q_M in a small region around the tune (Fig. 2) and near the next resonant frequency (Fig. 3). Note that the stochastic or chaotic layer appears first near the separatrix. The value for the driving amplitude is fixed and equal to $q = 1.0 \times 10^{-4}$. This is about an order of magnitude less than the critical value. In the succession of plots in Fig. 2 we see a continuous shrinking of the available regular phase space as the driving frequency increases. Note that there is a minimum in the available phase space at about $Q_M \simeq 4.5 \times 10^{-3}$. In the neigbourhood of this point the pendulum experiences a *nonlinear resonance* in good agreement with the theoretical prediction. We also observe a distortion in the regular trajectories that correspond to traces of KAM surfaces. This distortion is a result of our bad choise of variables since the proper study is done in an action-angle space. We also observe agreement with the theory in Fig. 3, although there the strength of the resonance is much lower.

4.2 Separating boundaries

The equation for the boundary that separates regular and chaotic motion is given by Eq. (50). In Fig. 4 we plot the driving torque q as a function of ω, the ratio of the driving frequency to the tune of the mashine. In Fig. 4a we have a log-log plot with $\alpha = 2$. In Figs. 4b, c, d we have $\alpha = 1, 2, 3$ respectively in semilog plots. In these figures the continuous line represents Eq. (50) wherease the dotted line its linearized version[1]. The chaotic regime is in the upper right hand side of the corresponding curves. Note that the frequency shift is substantial and the regular regime shrinks as α increases.

To test the validity of the new boundary we did simulations for $\omega = 0.25$ or $Q_M = 0.00132$. The resulting strobe plots are given in Fig. 5. We used the same initial conditions as in the previous plots. The approximate linear theory predicts a transition to essentially fully chaotic regime at about $q \simeq 4.0 \times 10^{-3}$ wherease the nonlinear theory at about $q \simeq 3.0 \times 10^{-3}$. In the

simulations this transition happens for q less than about 2.0×10^{-3}. Here again we see an improvement over the "linear boundary".

5 Conclusions

We presented an analytical and numerical study of the driven pendulum without resorting explicitly to Hamiltonian formalism and action-angle variables. We made some use of exact solutions and lowest order perturbative solutions to gain some intuition on the physics of the pendulum. From the preliminary comparisson with digital simulations we see that there is reasonably good agreement with the boundary formula derived in section (3.2). The frequency shift in the case of resonance is predicted also to few percent. In a following note we will give a more exhaustive comparison of theory and numerical simulations.

A Appendix

We give here a brief summary of the definitions and relations between some of the elliptic integrals and elliptic functions used in the text. The *normal elliptic integral of the first type* is defined as follows:

$$\int_0^u \frac{dt}{\sqrt{(1-t^2)(1-k^2t^2)}} = \int_0^\phi \frac{d\theta}{\sqrt{1-k^2sin^2\theta}} = \tag{52}$$

$$\int_0^u du' = u = sn^{-1}(y,k) = F(\phi,k) \tag{53}$$

with $y = sin\phi$ and $\phi = am(u,k)$. Note that the *sn* , or *sine amplitude* elliptic function is the inverse of the elliptic integral of the first kind and the *am* elliptic function its *amplitude*. With the introduction of two more Jacobian functions

$$cn^2 = 1 - sn^2, \tag{54}$$

$$dn^2 = 1 - k^2sn^2 \tag{55}$$

the remaining nine Jacobian functions are defined as ratios of the fundamental three.

Since occasionaly confusion arrises with the use of elliptic integrals and their inverses we discuss briefly the relation between $F(\phi,k)$, $sn(u,k)$ and $am(u,k)$ for real amplitudes and $0 \leq k \leq 1$. Start with

$$u = F(\phi,k) \tag{56}$$

Since ϕ is an angle, it variesin the range $-\infty < \phi < \infty$. We only need to deal with positive angles since $F(-\phi,k) = -F(\phi,k)$. The elliptic integral F is not a periodic function. However, as the angle ϕ increases (or decreases) by π, it essentially "repeats itself" since

$$F(m\pi \pm \phi,k) = 2mK \pm F(\phi,k) \tag{57}$$

with $K \equiv K(k) \equiv F(\pi/2,k)$. There is thus a monotonic increase of $2K$ for the dependent variable u everytime the angle increases by π. *If ϕ where to* represent an angle in a physical system such as a pendulum, then every time

the angle increases by 2π we pick an additional $4K$ in the quantity u. Note that $K(0) = \pi/2$ and thus

$$F(\phi, 0) = \phi \tag{58}$$

We also point out that only the values for the elliptic integral for $0 \leq \phi \leq \pi/2$ are important since $F(\phi + \pi/2, k) = 2K - F(\pi/2 - \phi, k)$. In other words $F(n\frac{\pi}{2}, k) = nK(k)$ and in the regions between these points u increases with alternating positive and negative curvature.

We now come to the *amplitude* function since

$$\phi = am(u, k) \tag{59}$$

Everytime u increases (or decreases) by $2K$, $am(u)$ increases (or decreases) by π. It is also a monotonic function that repeats itself with period $2K$.

Finally we are left with the sine amplitude $sn(u, k)$. Note that this is still an inverse of the elliptic integral $F(\phi, k)$. It is related to $am(u, k)$, but it is only *the periodic part of am* since it is defined as $y = sin\phi$, or

$$y = sin\phi = sn(u, k) \tag{60}$$

Note that because of the presence of a *sin* in the definition the periodicity of this function is now $4K$, since $u + 2K$ results to $\phi + \pi$ which only changes the sign in the $sin\phi$ function.

References

[1] S. G. Peggs, Hamiltonian theory of the E778 nonlinear dynamics experiment, SSC-175.

[2] P. F. Byrd and M. D. Friedman, Handbook of elliptic integrals for engineers and scientists, Springer, Berlin (1971).

[3] V. M. Kenkre and G. P. Tsironis, Nonlinear effects in quasielastic neutron scattering: Exact line-shape calculation for a dimer, Phys. Rev. **B35**, 1473 (1987).

[4] M. Abramowitz and I. S. Stegun, Handbook of mathematical functions, Dover, New York (1965).

Fig. 1a

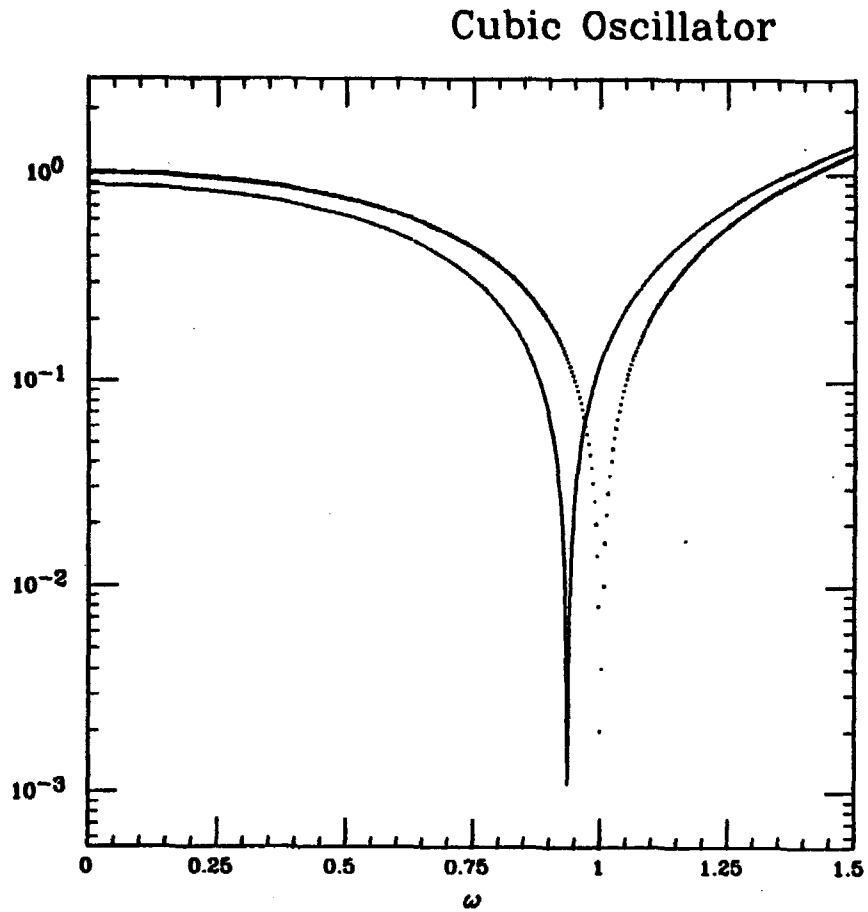

Fig. 1b

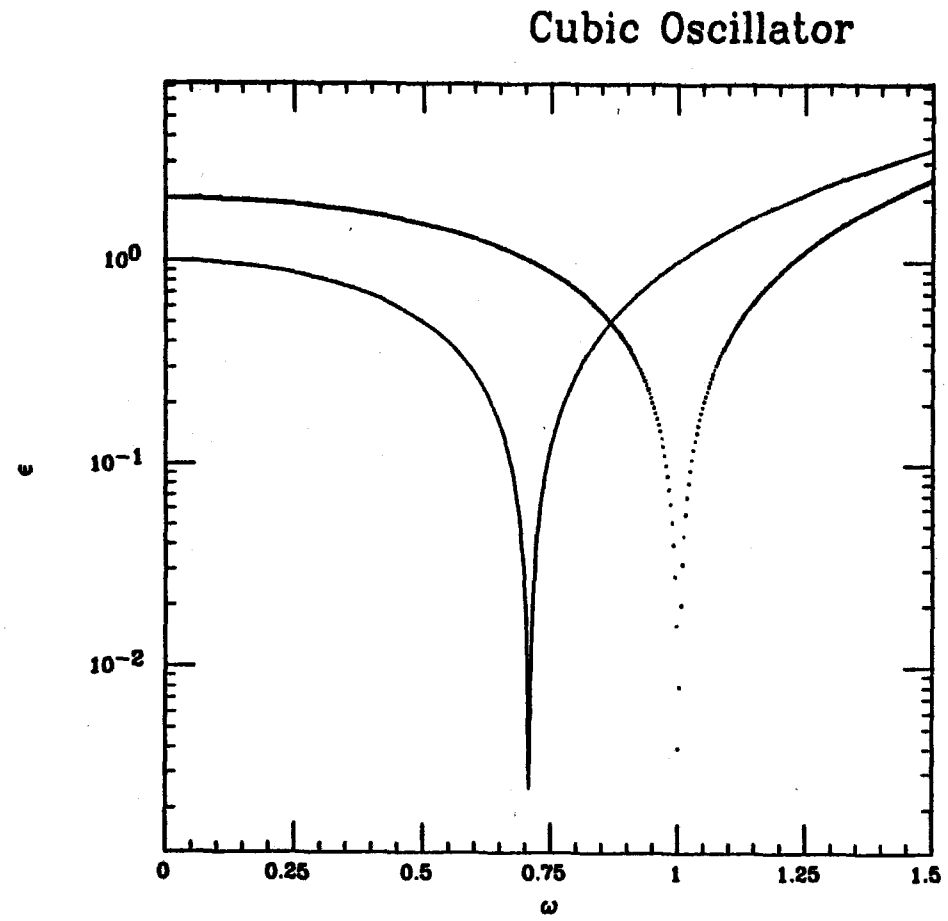
Cubic Oscillator
10^0
10^{-1}
10^{-2}
ϵ
0
0.25
0.5
0.75
1
1.25
1.5
ω

Fig. 2a

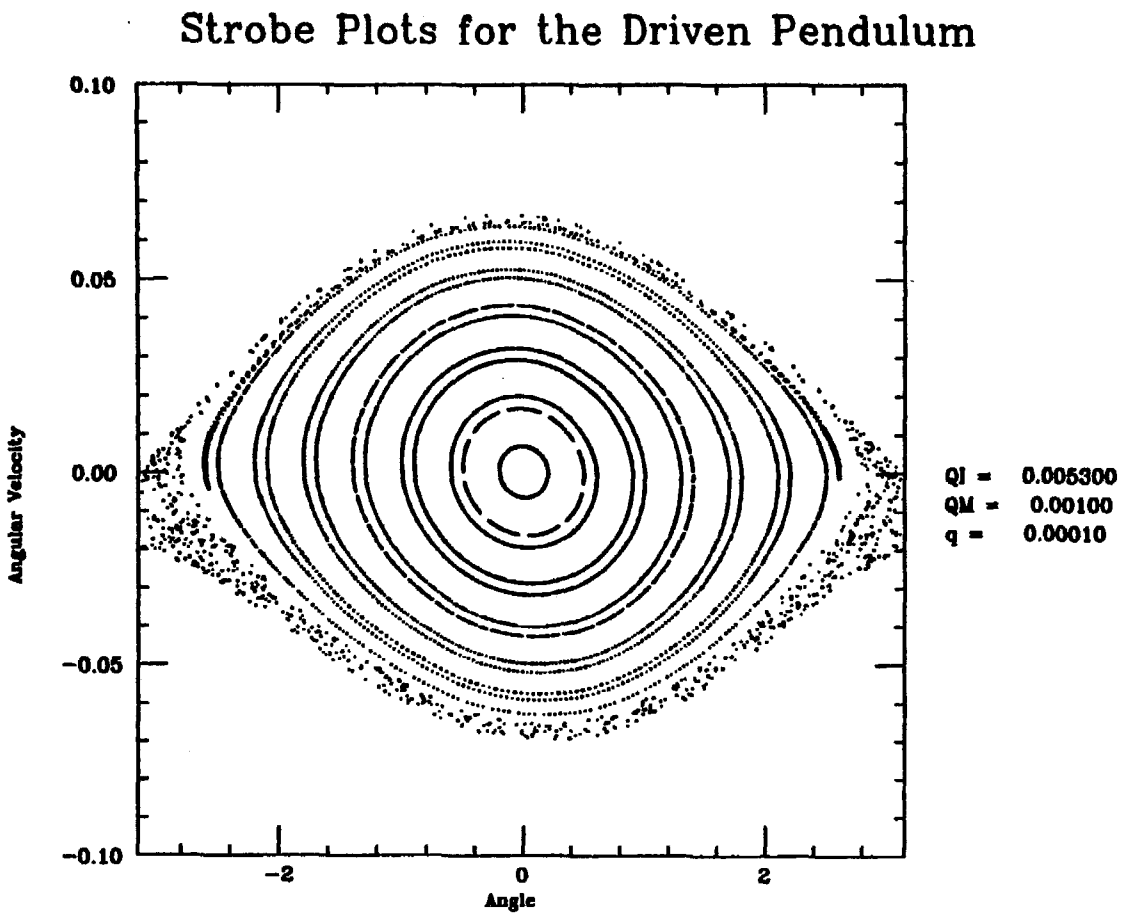
Strobe Plots for the Driven Pendulum
0.10
0.05
0.00
−0.05
−0.10
Angular Velocity
−2
0
2
Angle
QI = 0.005300
QM = 0.00100
q = 0.00010

Fig. 2b

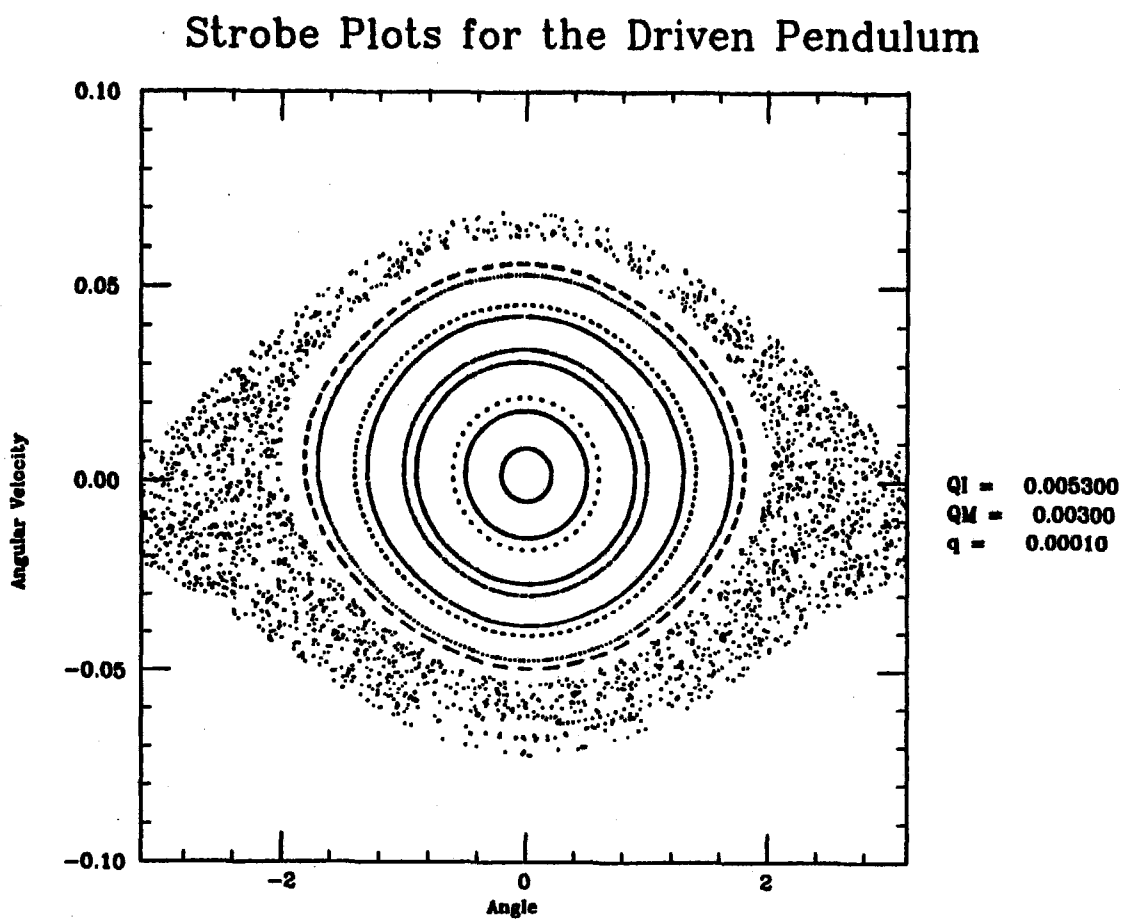
Strobe Plots for the Driven Pendulum
0.10
0.05
0.00
−0.05
−0.10
Angular Velocity
−2
0
2
Angle
QI = 0.005300
QM = 0.00300
q = 0.00010

Fig. 2c

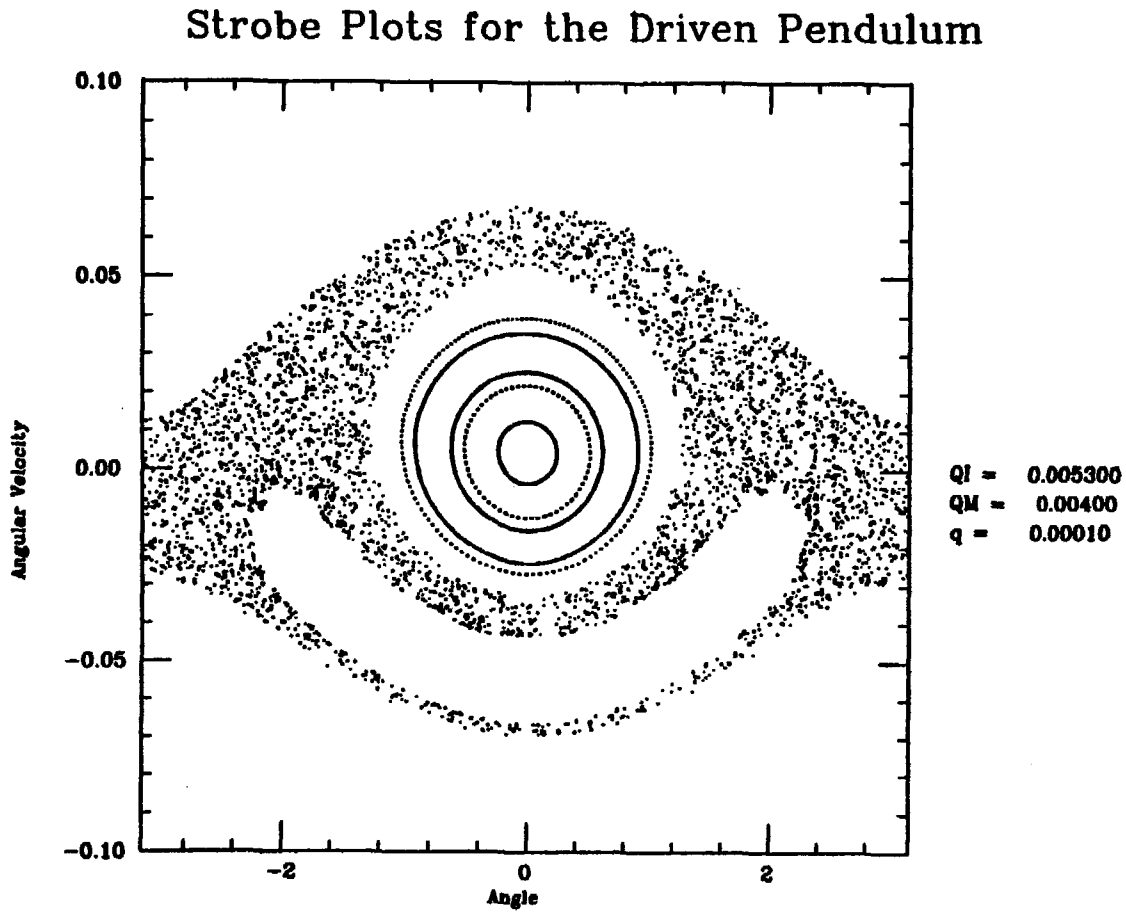
Strobe Plots for the Driven Pendulum
0.10
0.05
0.00
−0.05
−0.10
Angular Velocity
−2
0
2
Angle
QI = 0.005300
QM = 0.00400
q = 0.00010

Fig-2d

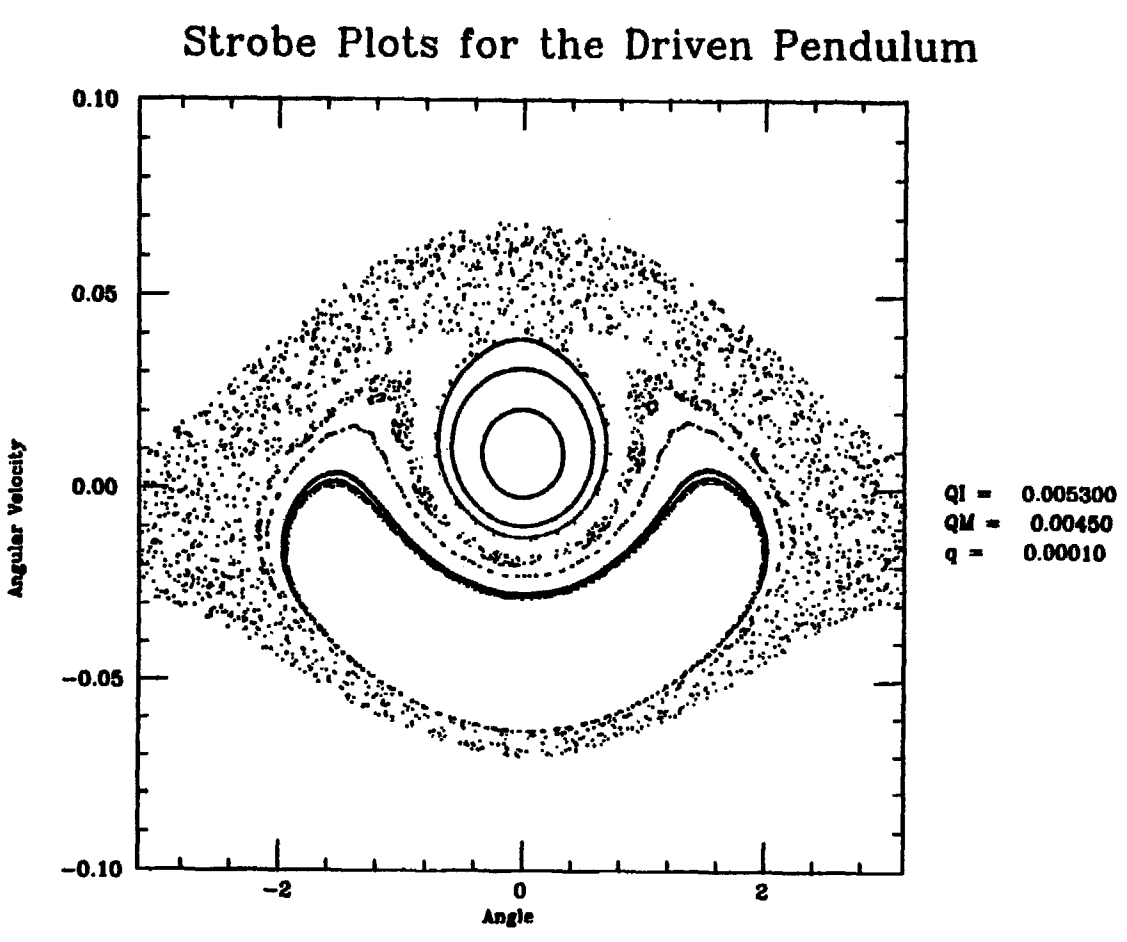
Strobe Plots for the Driven Pendulum
0.10
0.05
0.00
−0.05
−0.10
Angular Velocity
−2
0
2
Angle
QI = 0.005300
QM = 0.00450
q = 0.00010

Fig. 2

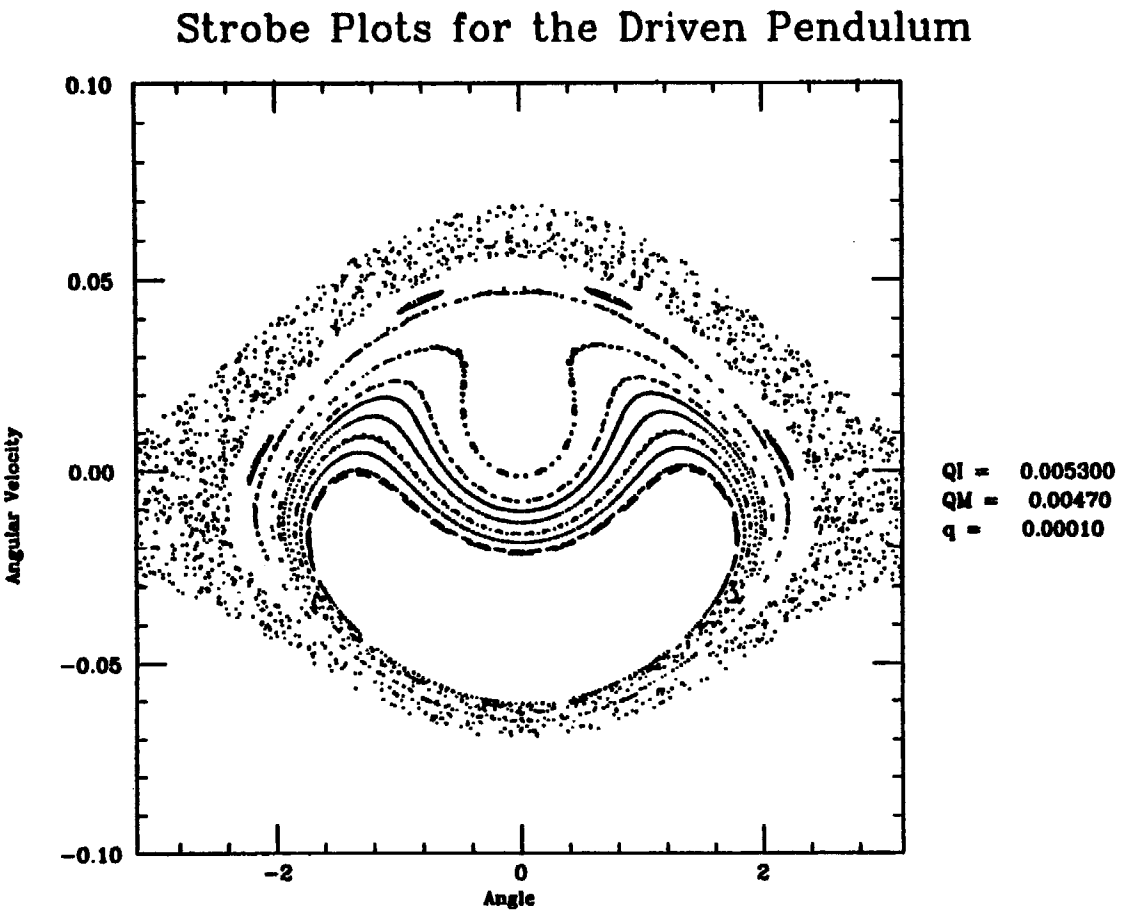
Strobe Plots for the Driven Pendulum
0.10
0.05
0.00
−0.05
−0.10
Angular Velocity
−2
0
2
Angle
QI = 0.005300
QM = 0.00470
q = 0.00010

Fig 2f

Strobe Plots for the Driven Pendulum

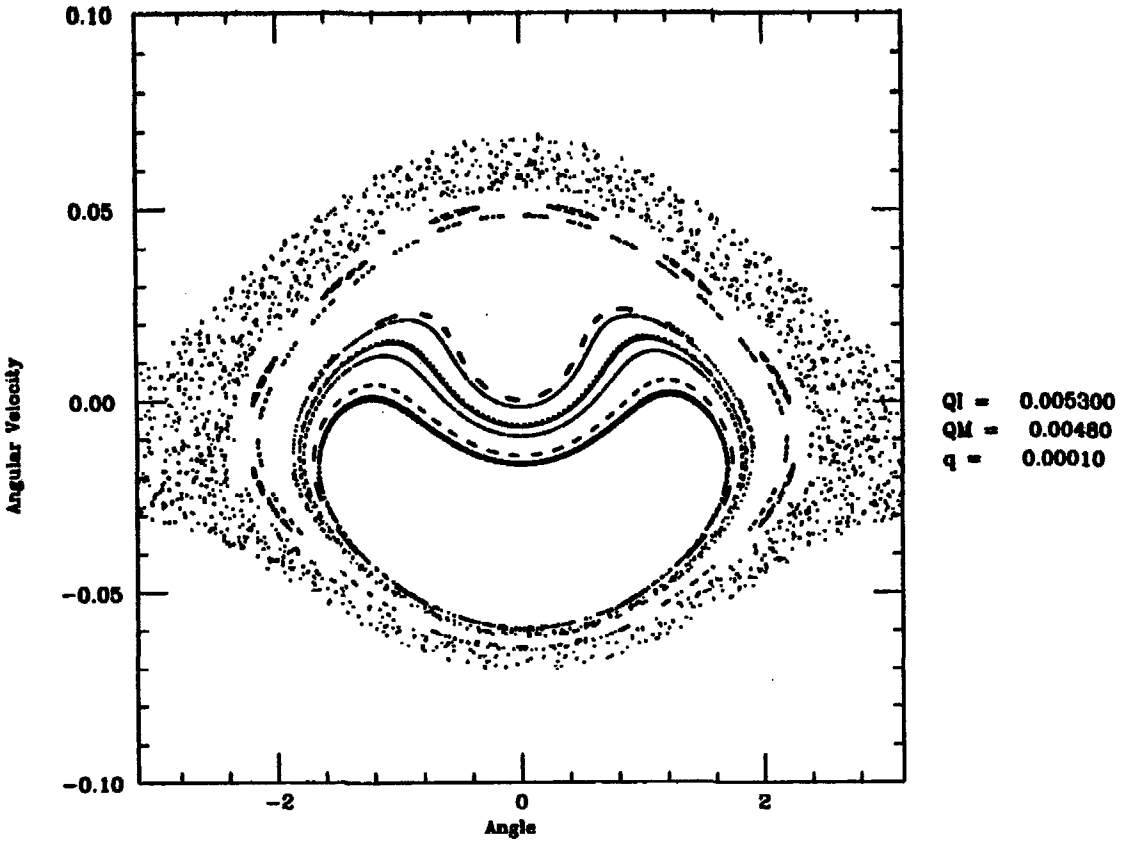

Fig. 2g

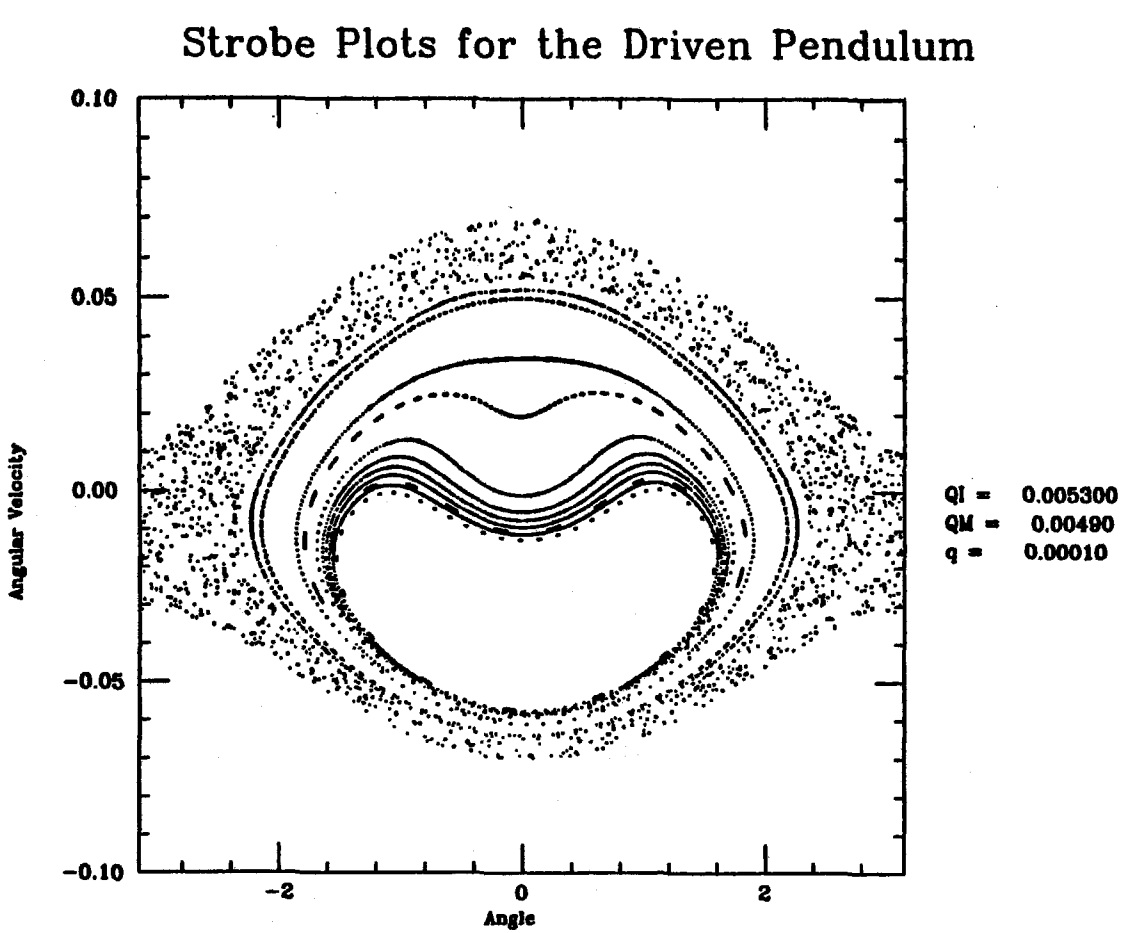
Strobe Plots for the Driven Pendulum
0.10
0.05
0.00
−0.05
−0.10
Angular Velocity
−2
0
2
Angle
QI = 0.005300
QM = 0.00490
q = 0.00010

Fig. 2a

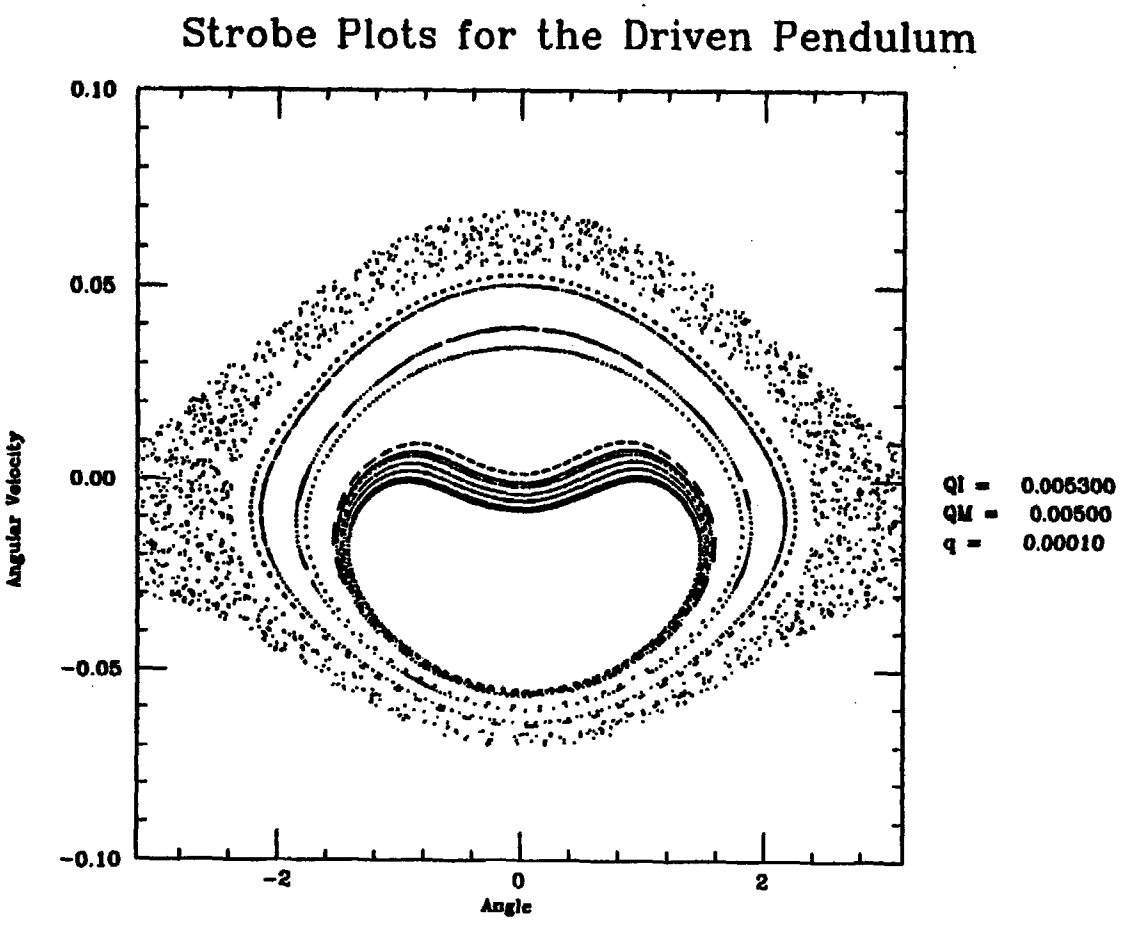
Strobe Plots for the Driven Pendulum
0.10
0.05
0.00
-0.05
-0.10
Angular Velocity
-2
0
2
Angle
QI = 0.005300
QM = 0.00500
q = 0.00010

Fig. 2c

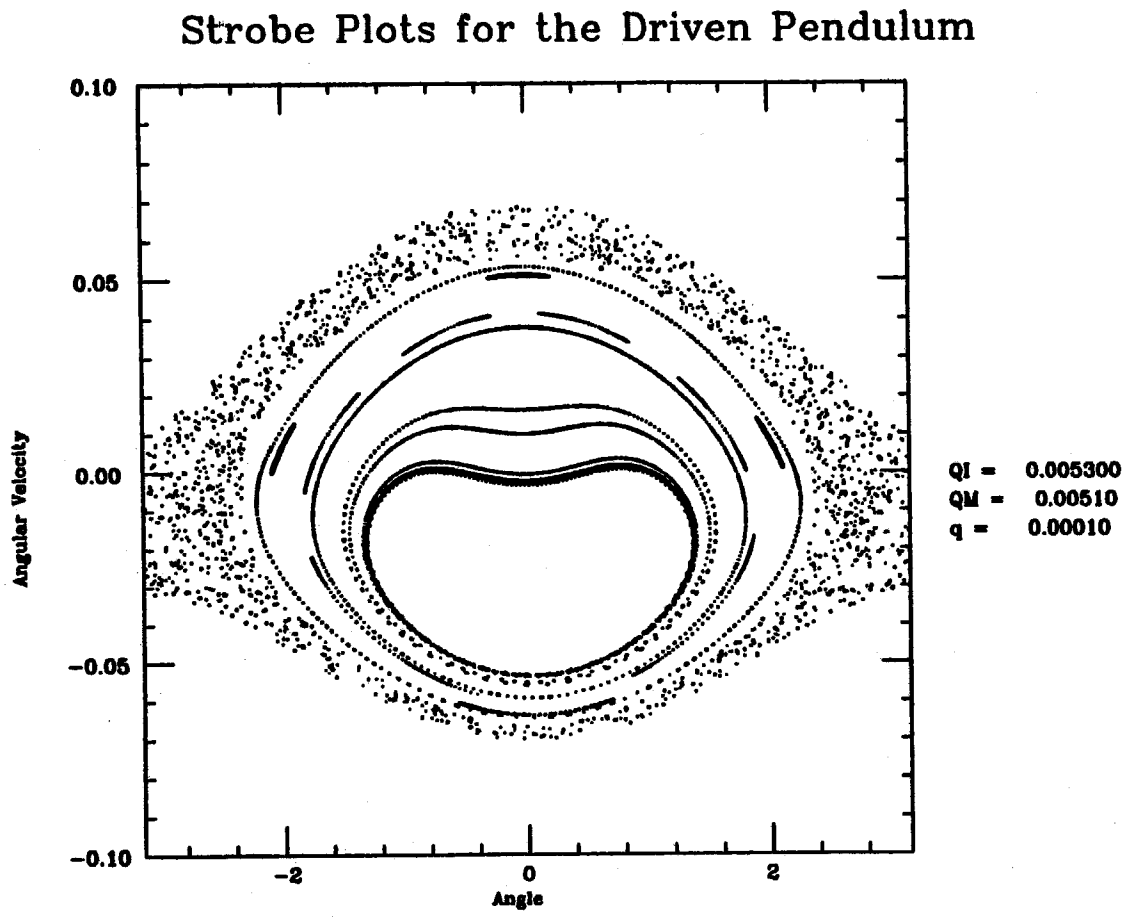
Strobe Plots for the Driven Pendulum
0.10
0.05
0.00
−0.05
−0.10
Angular Velocity
−2
0
2
Angle
QI = 0.005300
QM = 0.00510
q = 0.00010

Fig. 2j

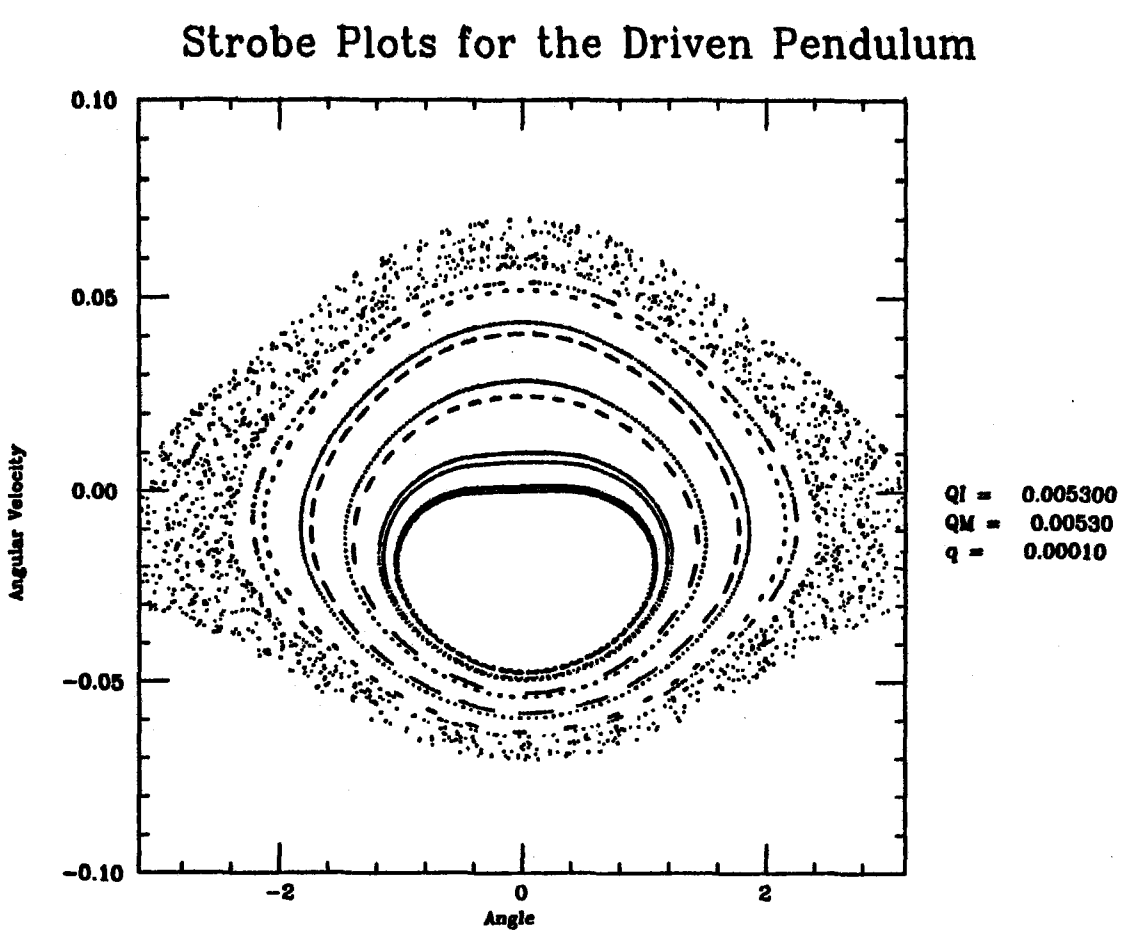
Strobe Plots for the Driven Pendulum
0.10
0.05
0.00
−0.05
−0.10
Angular Velocity
−2
0
2
Angle
QI = 0.005300
QM = 0.00530
q = 0.00010

Fig 3a

Strobe Plots for the Driven Pendulum

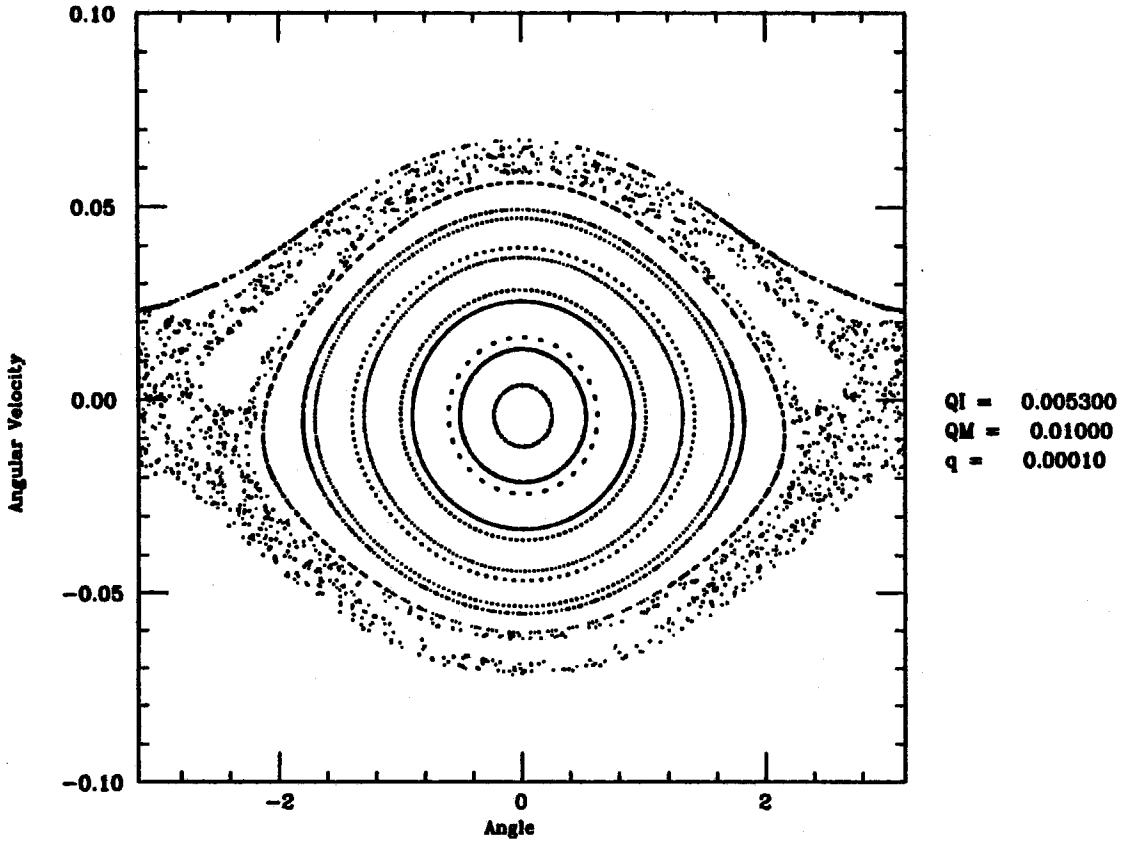

Fig. 5b

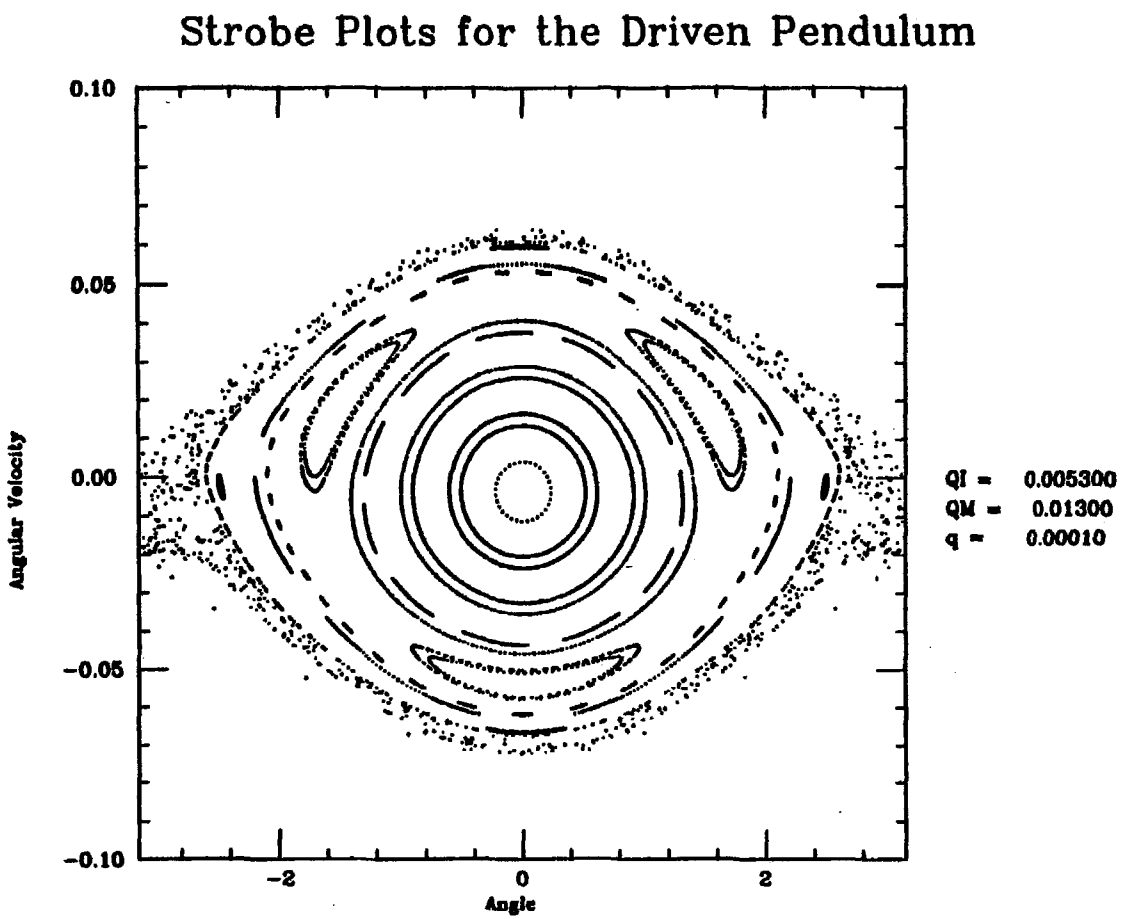
Strobe Plots for the Driven Pendulum
0.10
0.05
0.00
-0.05
-0.10
Angular Velocity
-2
0
2
Angle
QI = 0.005300
QM = 0.01300
q = 0.00010

Fig. 3c

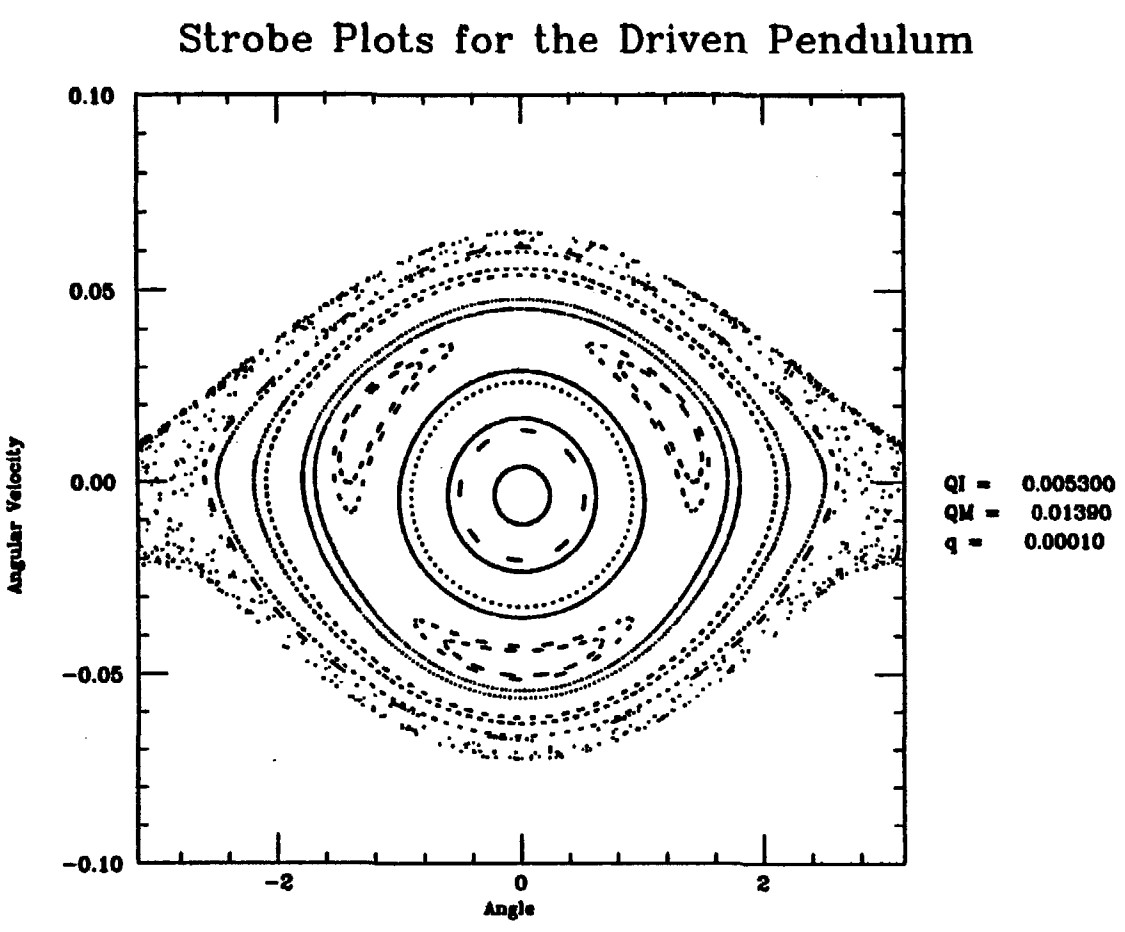
Strobe Plots for the Driven Pendulum
0.10
0.05
0.00
−0.05
−0.10
Angular Velocity
−2
0
2
Angle
QI = 0.005300
QM = 0.01390
q = 0.00010

Fig. 3d

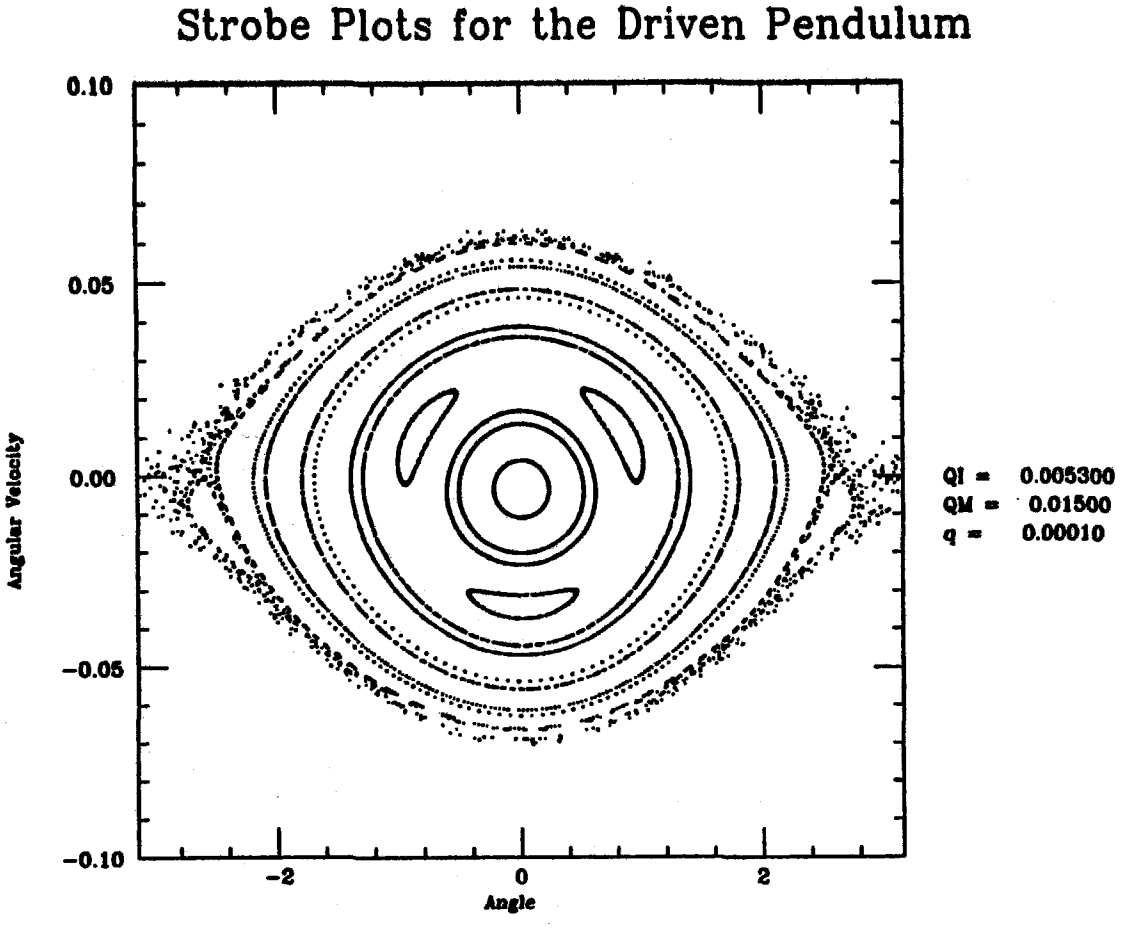
Strobe Plots for the Driven Pendulum
0.10
0.05
0.00
−0.05
−0.10
Angular Velocity
−2
0
2
Angle
QI = 0.005300
QM = 0.01500
q = 0.00010

Fig 4a

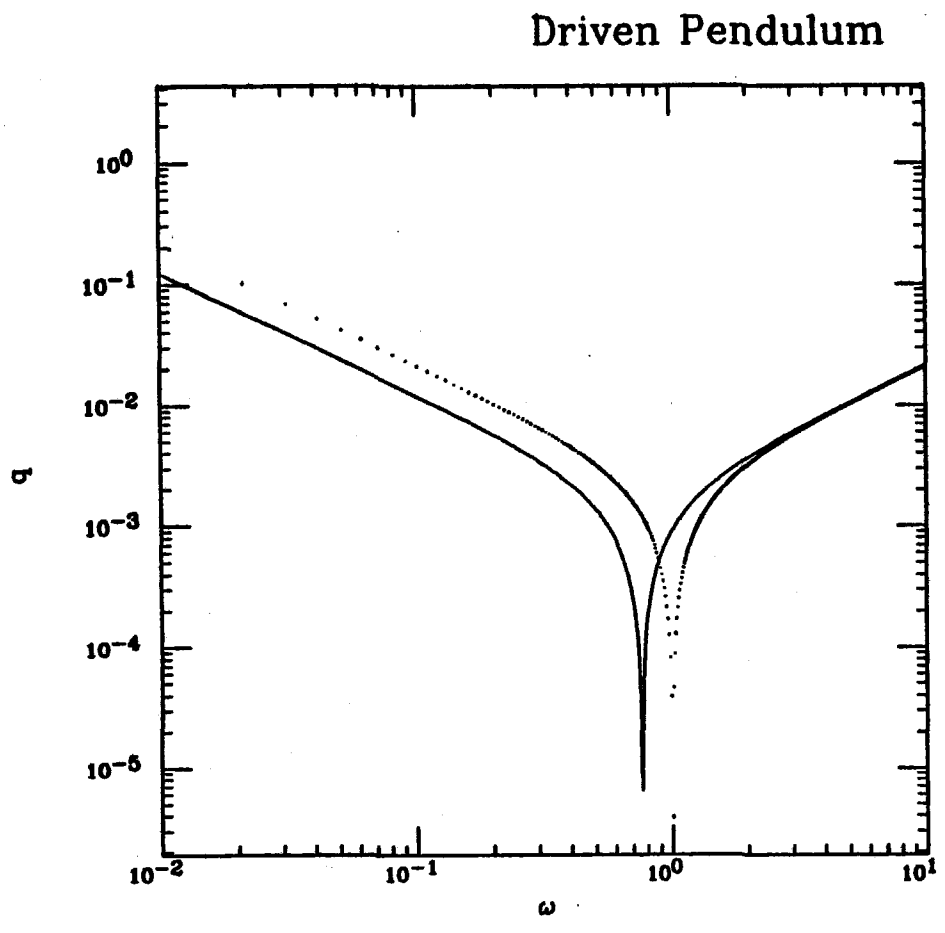

Fig. 4b

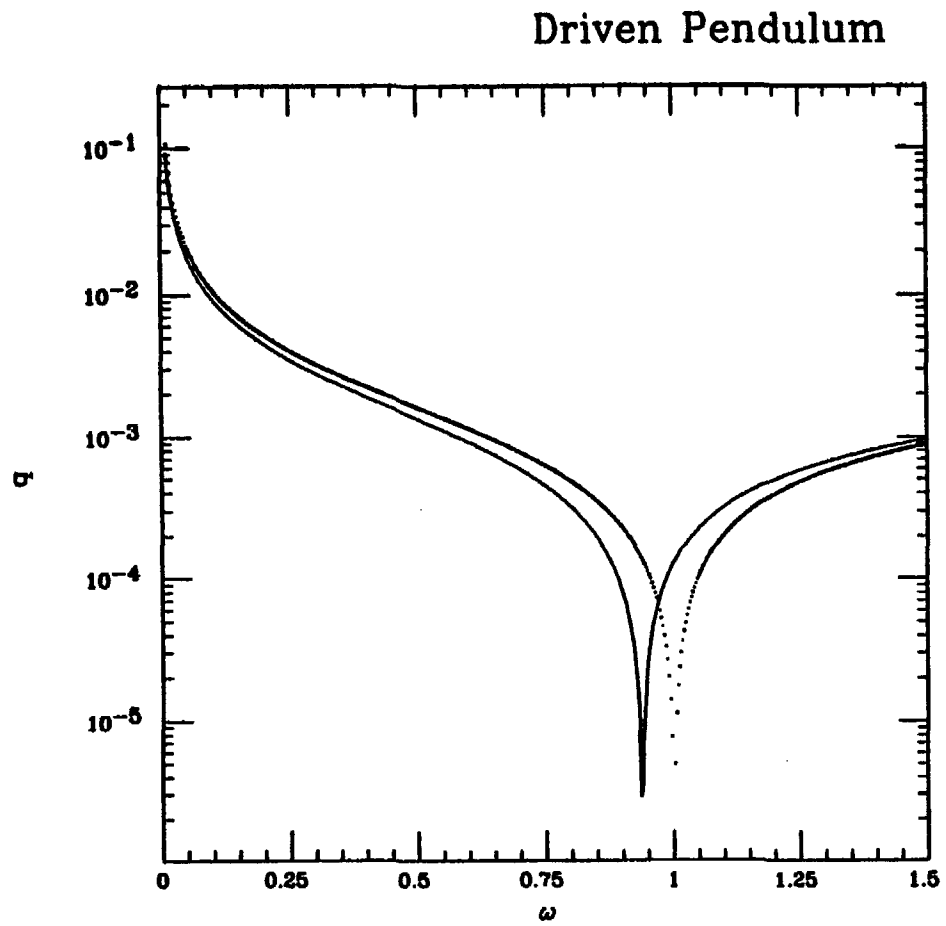

Fig. 4c

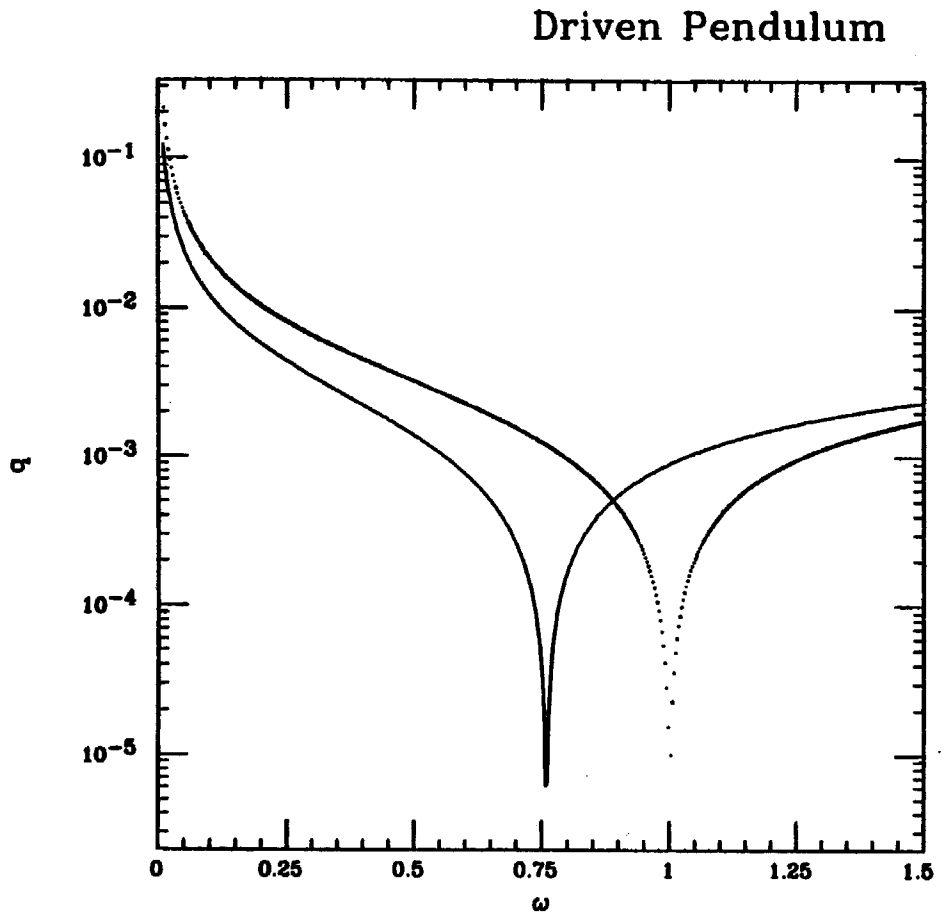

Fig. 4d

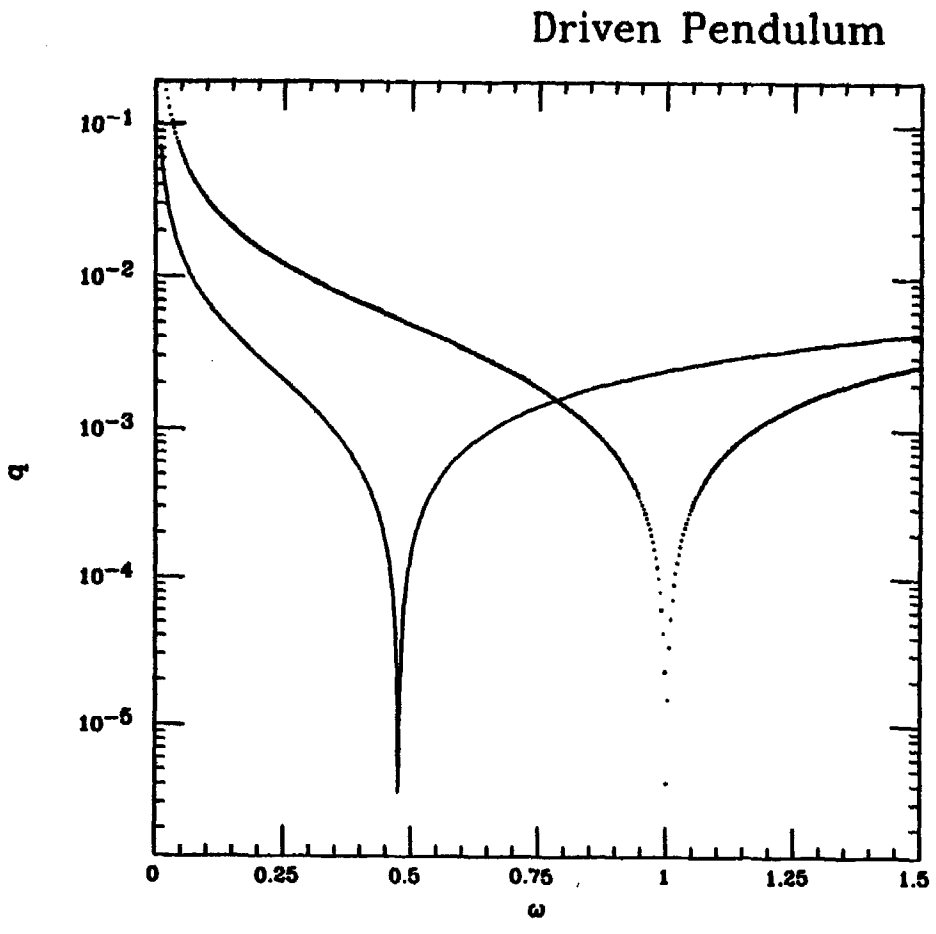

Fig. 5a

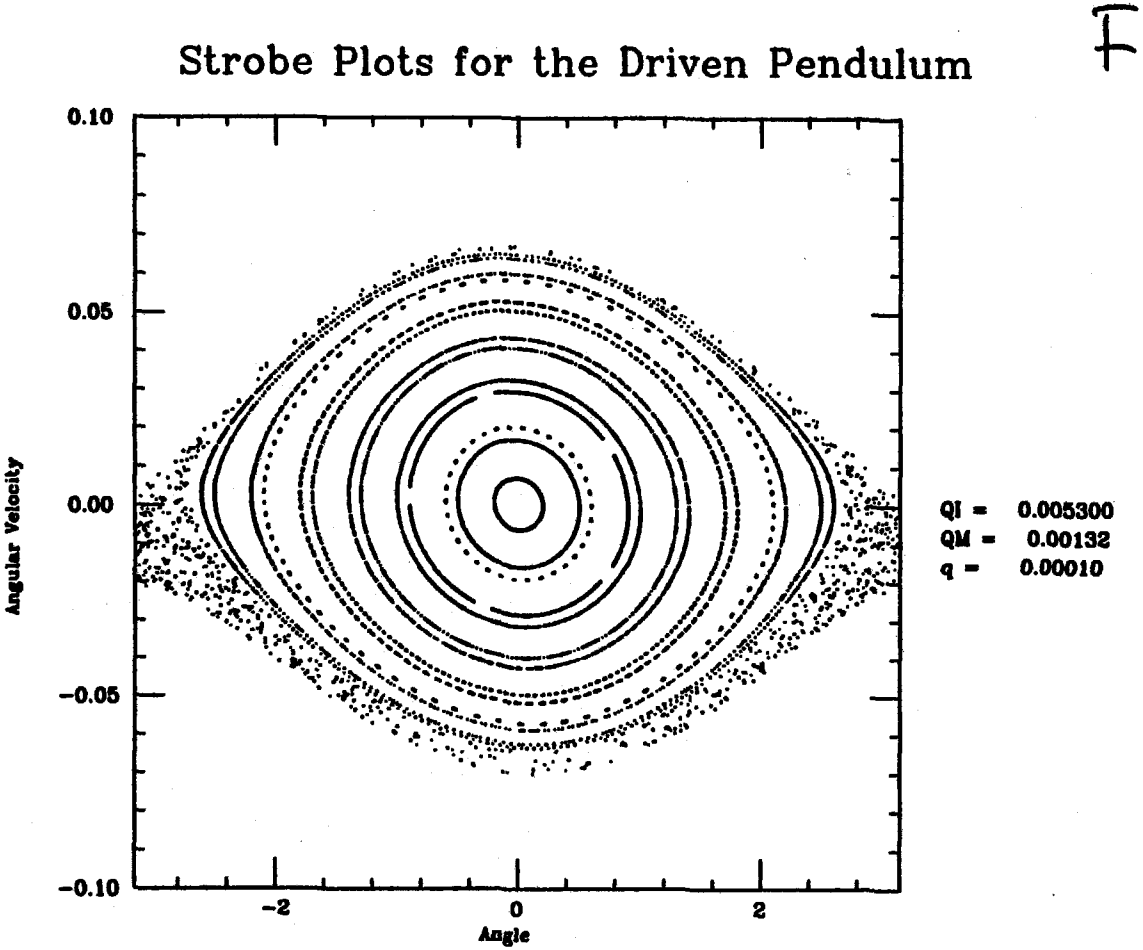
Strobe Plots for the Driven Pendulum
0.10
0.05
0.00
−0.05
−0.10
Angular Velocity
−2
0
2
Angle
QI = 0.005300
QM = 0.00132
q = 0.00010

Fig. 5b

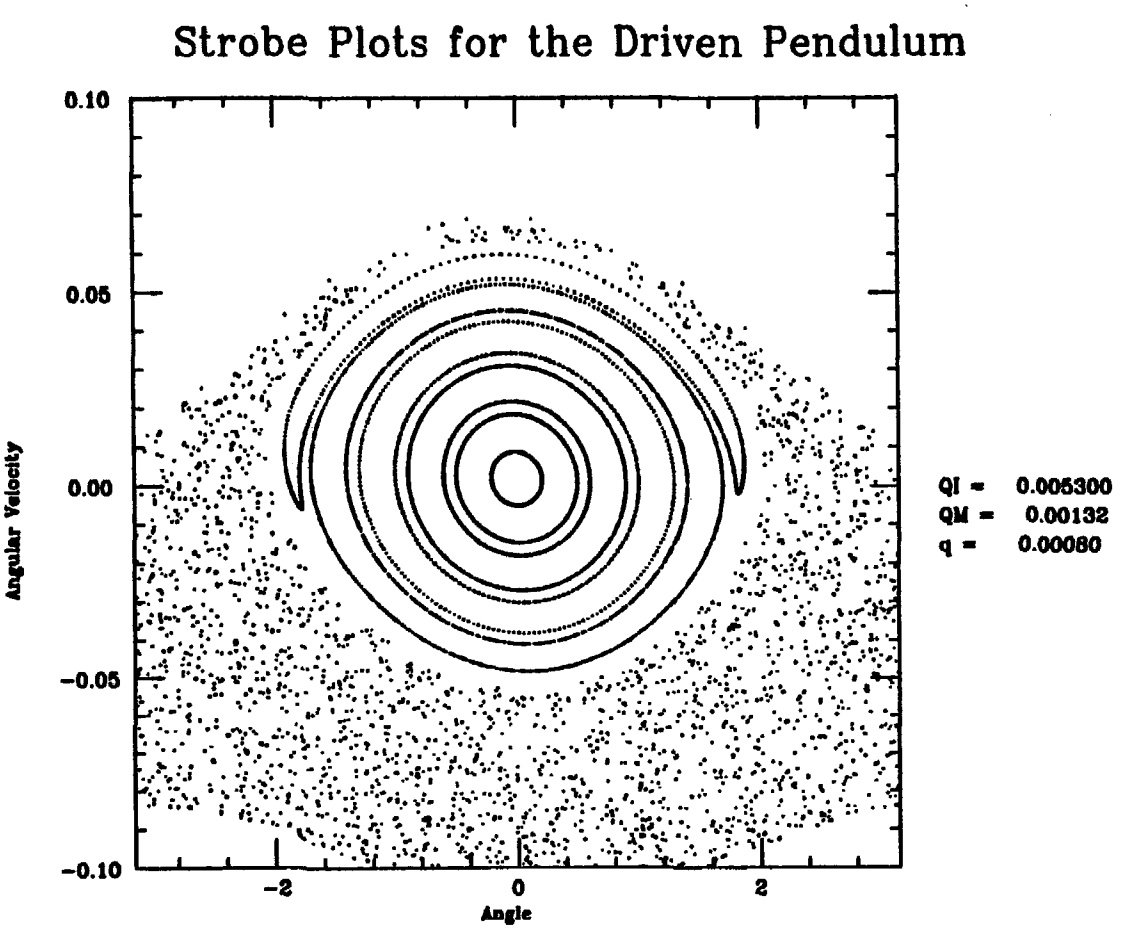
Strobe Plots for the Driven Pendulum
0.10
0.05
0.00
−0.05
−0.10
Angular Velocity
−2
0
2
Angle
QI = 0.005300
QM = 0.00132
q = 0.00080

Fig. 5c

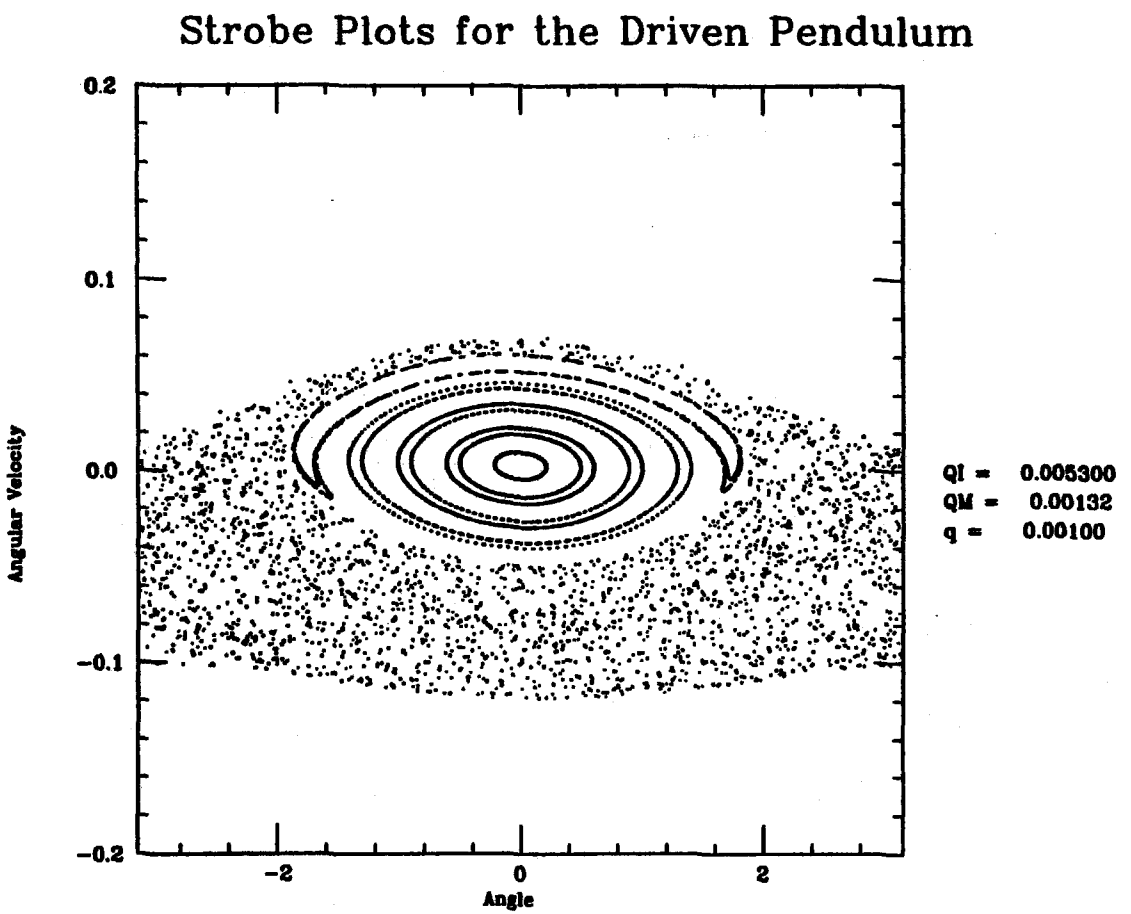
Strobe Plots for the Driven Pendulum
0.2
0.1
0.0
−0.1
−0.2
Angular Velocity
−2
0
2
Angle
QI = 0.005300
QM = 0.00132
q = 0.00100

Fig. 5d

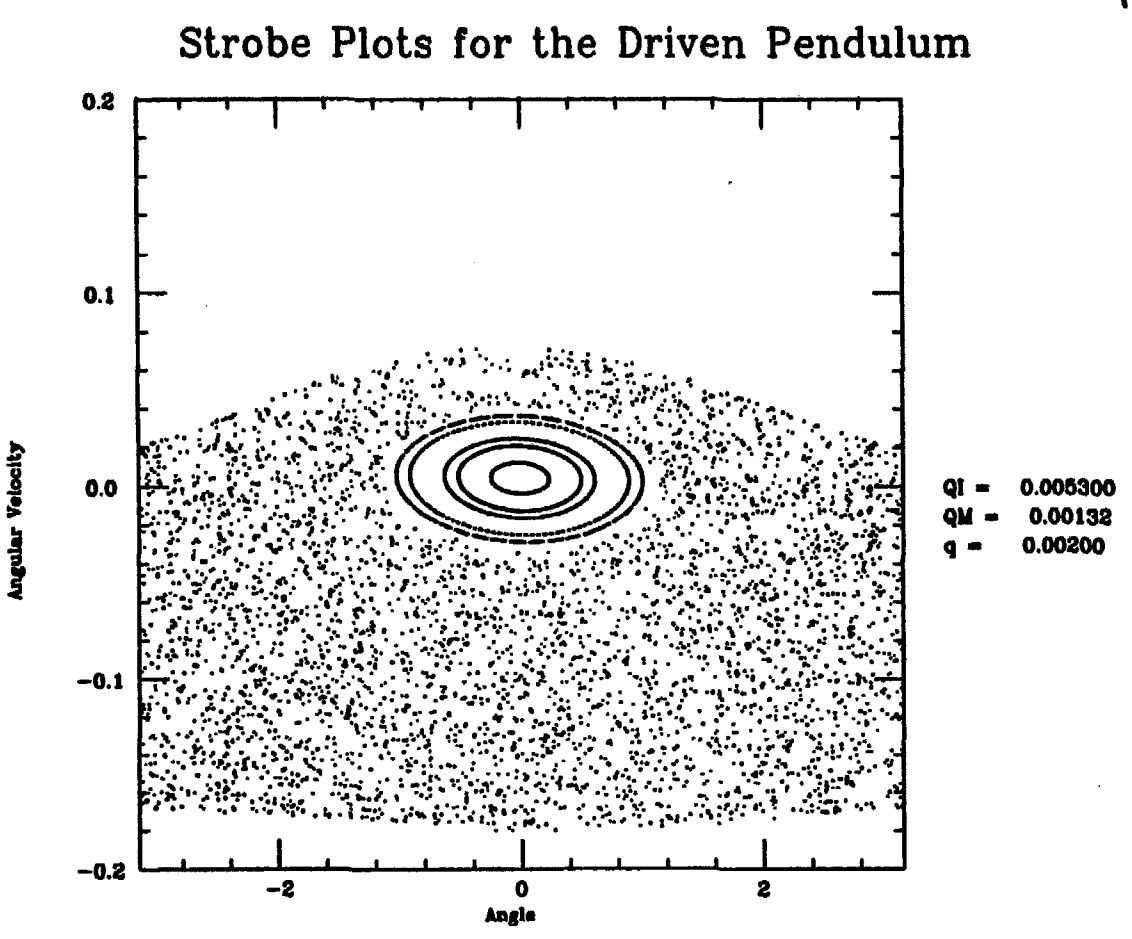
Strobe Plots for the Driven Pendulum
0.2
0.1
0.0
−0.1
−0.2
Angular Velocity
−2
0
2
Angle
QI = 0.005300
QM = 0.00132
q = 0.00200

Fig. 5c

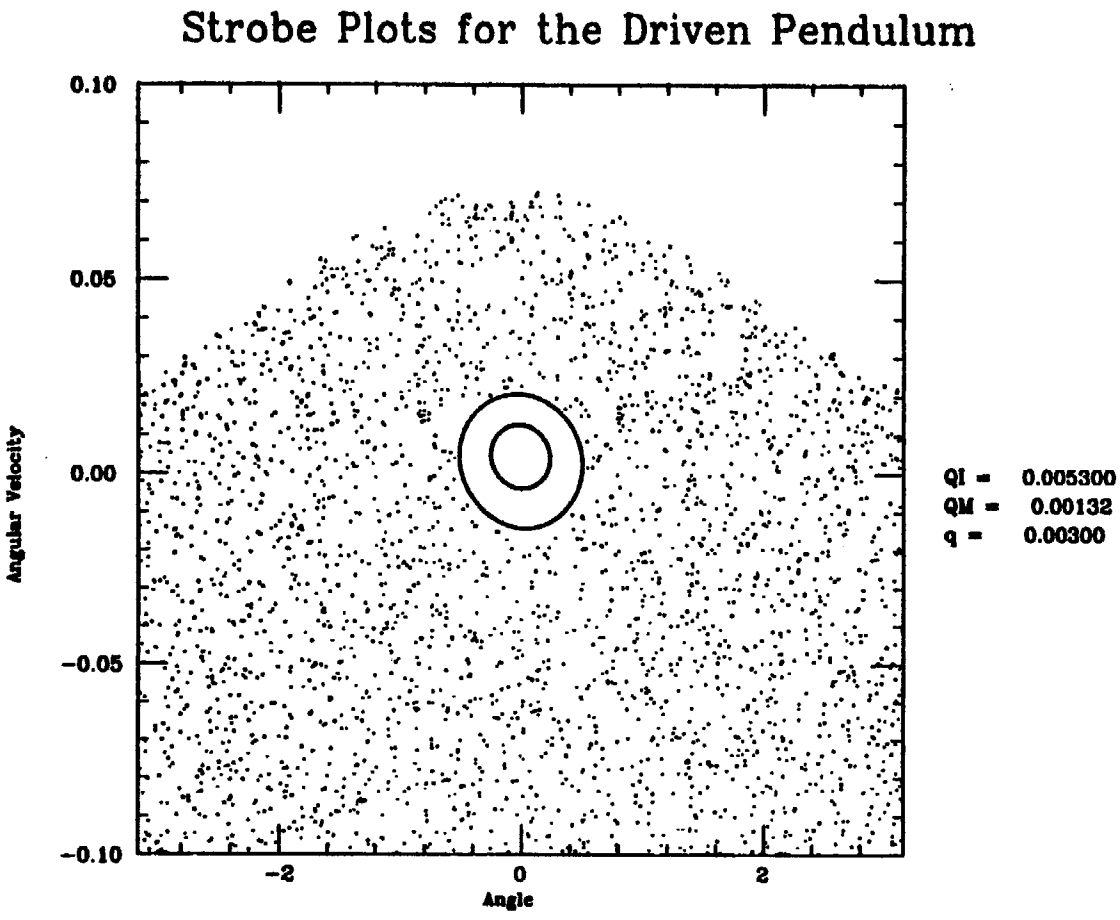
Strobe Plots for the Driven Pendulum
0.10
0.05
0.00
−0.05
−0.10
Angular Velocity
−2
0
2
Angle
QI = 0.005300
QM = 0.00132
q = 0.00300